INVITED PAPER

Affective Brain–Computer Interfaces (aBCIs): A Tutorial

This tutorial guides the reader into the basics of brain–computer interfaces (BCIs) leading into "closed-loop" affective BCIs that include the chain from analysis to brain stimulation.

By Dongrui Wu, *Fellow IEEE*, Bao-Liang Lu, *Fellow IEEE*, Bin Hu, *Fellow IEEE*, and Zhigang Zeng, *Fellow IEEE*

ABSTRACT | A brain–computer interface (BCI) enables a user to communicate directly with a computer using only the central nervous system. An affective BCI (aBCI) monitors and/or regulates the emotional state of the brain, which could facilitate human cognition, communication, decision-making, and health. The last decade has witnessed rapid progress in aBCI research and applications, but there does not exist a comprehensive and up-to-date tutorial on aBCIs. This tutorial fills the gap. It introduces first the basic concepts of BCIs and then, in detail, the individual components in a closed-loop aBCI system, including signal acquisition, signal processing, feature extraction, emotion recognition, and brain stimulation. Next, it describes three representative applications of aBCIs, i.e., cognitive workload recognition, fatigue estimation, and depression diagnosis and treatment. Several challenges and opportunities in aBCI research and applications, including brain signal acquisition, emotion labeling, diversity and size of aBCI datasets, algorithm comparison, negative transfer in emotion recognition, and privacy protection and security of aBCIs, are also explained.

KEYWORDS | Affective computing; brain–computer interface (BCI); emotion recognition; emotion regulation; machine learning.

Manuscript received 4 October 2022; revised 21 April 2023; accepted 11 May 2023. Date of publication 31 May 2023; date of current version 11 October 2023. This work was supported in part by the STI 2030—Major Project 2021ZD0201300 and in part by the Hubei Province Funds for Distinguished Young Scholars under Grant 2020CFA050. *(Corresponding authors: Bin Hu; Zhigang Zeng.)*

Dongrui Wu and **Zhigang Zeng** are with the Key Laboratory of the Ministry of Education for Image Processing and Intelligent Control, School of Artificial Intelligence and Automation, Huazhong University of Science and Technology, Wuhan 430074, China (e-mail: drwu@hust.edu.cn; zgzeng@hust.edu.cn).

Bao-Liang Lu is with the Department of Computer Science and Engineering, Shanghai Jiao Tong University, Shanghai 200240, China (e-mail: bllu@sjtu.edu.cn).

Bin Hu is with the Institute of Engineering Medicine, Beijing Institute of Technology, Beijing 100811, China (e-mail: bh@bit.edu.cn).

Digital Object Identifier 10.1109/JPROC.2023.3277471

I. INTRODUCTION

Affects, including moods and emotions, are pervasive in our everyday life and essential in human cognition, communication, and decision-making [1]. They are also very important in human–machine interactions. For example, one of the founding fathers of artificial intelligence, Prof. Alan Minsky [2], argued early in 1988 in his seminal book *The Society of Mind* that "the question is not whether intelligent machines can have any emotions, but whether machines can be intelligent without any emotions."

Affective computing, first proposed by Prof. Rosalind Picard in 1995 [3], is "computing that relates to, arises from, or influences emotions." It quickly became an interdisciplinary research area of computer science, psychology, cognitive science, and so on. As shown in Fig. 1, the biannual International Conference on Affective Computing and Intelligent Interaction (ACII) was initiated in 2005 and the affiliated aBCI Workshop in 2009. A dedicated journal, IEEE Transactions on Affective Computing, was established in 2010. The Association for the Advancement of Affective Computing (AAAC) was founded in 2011. As of April 20, 2023, on Google Scholar, about 1200 researchers choose affective computing as one of their areas of interest, and about 82 000 publications included "affective computing" in their titles or texts.

Humans can recognize and display emotions through facial expressions [4], speech [5], gestures [6], texts [7], and their combinations [8]. These are also important modalities in affective computing. Physiological signals, e.g., electroencephalogram (EEG), functional magnetic resonance imaging (fMRI), functional near-infrared spectroscopy (fNIRS), electrocardiogram (ECG), eye movement, blood pressure, skin temperature, and respiration, have also been used in affective computing [9], [10]. Compared with other modalities, physiological signals are more difficult to disguise and, hence, may reflect more

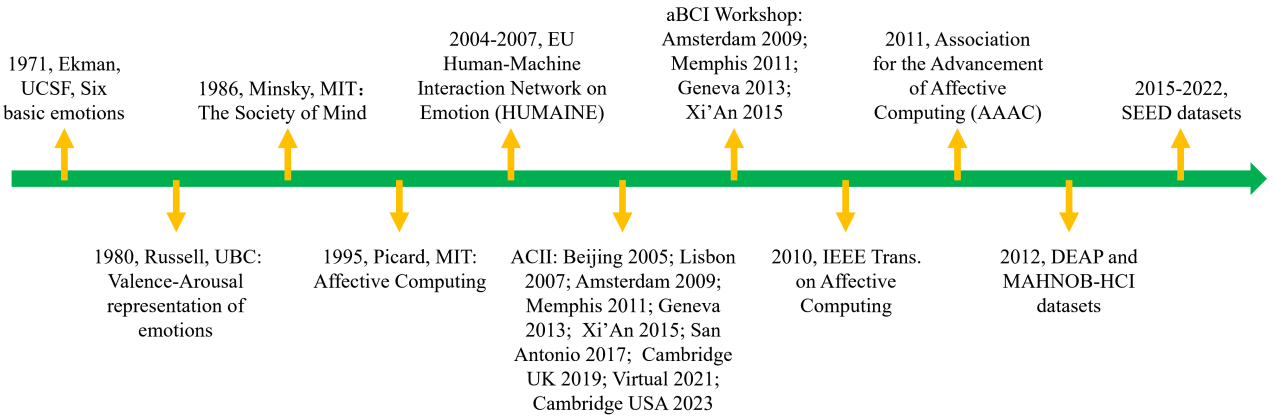

Fig. 1. ***Important events in the history of aBCIs.***

authentic emotions. Brain signals, particularly EEG, are popular in physiological signal-based affective computing, perhaps because they directly measure the state of the brain, where emotions originate.

Brain signals are also the input signals in brain–computer interfaces (BCIs) [11], which enable a user to communicate directly with a computer using only the central nervous system. BCIs have found applications in neural rehabilitation [12], text input [13], gaming [14], emotion recognition [15], mental fatigue evaluation [16], vigilance estimation [17], speech synthesis [18], sentence decoding [19], movement and touch functionality recovery [20], [21], robot control [22], [23], and so on.

According to the input signal source, there are three types of BCIs [24], [25].

1) *Noninvasive BCIs*, where brain signals are recorded on the scalp. EEG is the most popular input to noninvasive BCIs due to its safety, low cost, and convenience.
2) *Invasive BCIs*, which surgically implant sensor arrays or electrodes into the cortex to record and decode brain signals, and/or stimulate the brain.
3) *Partially invasive BCIs*, which surgically place the sensors between the skull and the cortex.

An affective BCI (aBCI) [26] monitors and/or regulates the emotional state of the brain. It has been attracting rapidly increasing research interests recently, as demonstrated in Fig. 2, which shows the number of publications per year returned by query *Emotion OR Affect "brain computer interface"* on Google Scholar.

The flowchart of a closed-loop aBCI system is depicted in Fig. 3. It consists of signal acquisition, signal processing, feature extraction, emotion recognition, and/or brain stimulation. Most aBCIs so far are noninvasive BCIs, especially when brain stimulation is not included.

Compared with a traditional motor BCI, in which Shanechi [27] "uses a mathematical algorithm termed a "decoder" to estimate the user's intended movement state from neural activity, uses the decoded movement to control an external actuator (prosthetic device), and provides sensory and reward feedback to the user," an aBCI has two important characteristics.

1) *Multimodal inputs:* In addition to EEG, physiological signals, such as eye movements, and nonphysiological signals, such as facial expressions and speech, are also frequently used in aBCIs for more accurate emotion recognition. In contrast, classical noninvasive motor imagery-based BCIs [28] usually use solely EEG signals.
2) More factors to be considered, e.g., the subject's age, gender, and/or cultural/education background. Otherwise, it may be difficult to effectively induce the intended emotions. For example, the video clips used in aBCI experiments should ideally be different for teenagers and the elderly. These additional factors are generally not very important for motor BCIs.

Rapid progress has been made in each aBCI block in Fig. 3 in the past few decades, but there does not exist a comprehensive and up-to-date tutorial on them. This tutorial fills the gap by introducing these individual components in detail. Among the three input brain signals (EEG, fMRI, and fNIRS), fMRI and fNIRS, perhaps due to

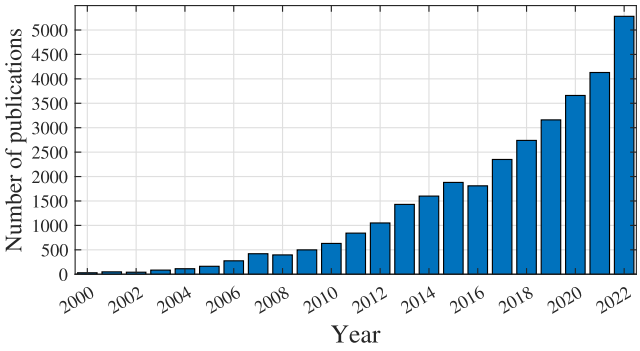

Fig. 2. ***Number of publications per year, returned by query* Emotion OR Affect "brain computer interface" *on Google Scholar on April 15, 2023.***

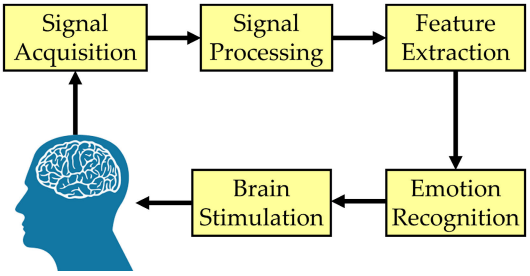

Fig. 3. *Flowchart of a closed-loop aBCI system.*

their high cost, larger sizes, and shorter history, are used less frequently than EEG in aBCIs. For example, a Google Scholar search of "EEG emotion" in the title on April 20, 2023, returned 2260 articles, whereas "fMRI emotion" returned 523 articles, and "fNIRS emotion" returned 28 results. In addition, many studies in the latter two categories are on the evaluation of brain activities in different emotional states, instead of emotion recognition. A Web of Science search on April 20, 2023, revealed that, among all 733 IEEE TRANSACTIONS ON AFFECTIVE COMPUTING publications so far, 79 are on EEG, two on fMRI, and none on fNIRS. Thus, fMRI- and fNIRS-based aBCIs are only briefly introduced in this tutorial. The focus is on EEG-based aBCIs.

The remainder of this tutorial is organized as follows. Sections II–VI describe in detail the individual components in Fig. 3, i.e., signal acquisition, signal processing, feature extraction, emotion recognition, and brain stimulation, respectively. Section VII introduces applications of aBCIs. Section VIII points out challenges and future research directions in aBCIs. Finally, Section IX draws conclusions.

II. SIGNAL ACQUISITION IN aBCIs

Different brain signals have been used in aBCIs, e.g., EEG, fMRI, and fNIRS. They are also frequently recorded together with other physiological signals, e.g., ECG and eye movement, and video and speech, for multimodal and more accurate aBCIs. This section introduces how typical aBCI experiments are performed, and how the brain signals are acquired.

A. Emotion Representation

Emotions can be represented using categories, e.g., Ekman's six basic emotions [29] (anger, disgust, fear, happiness, sadness, and surprise), or continuously in the 2-D space of arousal and pleasure (or valence) [30], or the 3-D space of arousal, pleasure (or valence), and dominance [31], as shown in Fig. 4. Both categorical and continuous emotions have been used in aBCIs.

B. Emotion Elicitation

Most aBCI experiments were performed in controlled laboratory environments, using deliberately designed settings to elicit specific emotions of the subjects, and recording the brain and other physiological signals simultaneously. For example, a "happy" movie clip rated by multiple evaluators is supposed to elicit a happy emotion from the subject.

Unlike other classical BCI paradigms, e.g., motor imagery [32], event-related potentials [33], and steady-state visual evoked potentials [34], aBCI experiments are more difficult to perform due to the following reasons.

1) Music or videos are frequently used to elicit specific emotions; thus, the emotions of the music or videos need to be evaluated first. Since emotion is very subtle and has large individual differences, multiple evaluators are needed for each music or video, which is labor-intensive. For example, in the popular DEAP dataset [35], 14–16 volunteers were recruited to evaluate the arousal, valence, and dominance values of each music video.
2) It takes some time for music or video to influence the emotion of a user, so an aBCI data trial is generally longer than a trial in other BCI paradigms. For example, a steady-state visual evoked potential [13] trial may be less than a second, and motor imagery [32] or event-related potential [33] trial may take only a few seconds, whereas an aBCI trial may take a couple of minutes. Thus, collecting aBCI data is time-consuming.
3) Usually, aBCI experiments require the subjects to concentrate on the emotional media to elicit the intended emotion, which may quickly result in fatigue. Thus, an aBCI experiment cannot last too long. As each aBCI trial may take a couple of minutes, this further reduces the number of trials per subject in an aBCI experiment.

C. Input Signals

Different brain signals, e.g., EEG, fMRI, and fNIRS, have been used in aBCIs, with EEG being the most popular.

EEG signals can be acquired by an EEG headset from the scalp [36]. A typical EEG headset includes tens of channels (electrodes), labeled according to the international 10-20 or 10-10 system, as shown in Fig. 5. The letters on a

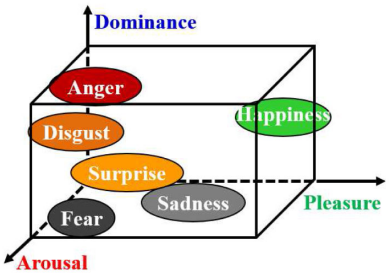

Fig. 4. *Ekman's six basic emotions in the 3-D space of arousal, pleasure, and dominance.*

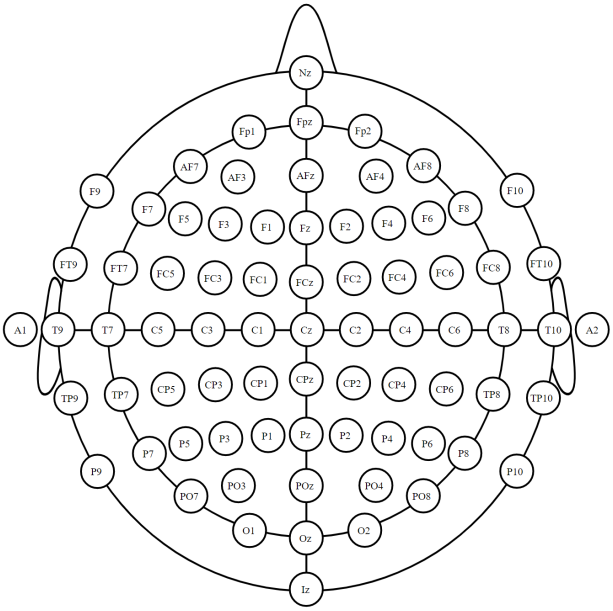

Fig. 5. *Electrode labels and locations of an EEG headset according to the international 10-10 system. Nz: nose; A: ear lobe; F: frontal; C: central; P: parietal; O: occipital; T: temporal; Fp: frontal polar; and z: zero.*

label indicate the lobe location, and the number (index) indicates how far away the electrode is from the center of the brain: the index increases as the electrode moves away from the central. The odd indices are on the left, and the even indices are on the right.

The typical amplitude of EEG is between 5 and 300 μV, and the highest useful frequency is usually below 100 Hz [37]. EEG signals can be partitioned into different frequency bands, reflecting different emotions or brain states, as summarized in Table 1.

Not all EEG frequency bands and channels contribute equally to emotion recognition. Ray and Cole [40] found that EEG alpha activity reflects attentional demands, whereas beta activity reflects emotional and cognitive processes. Furthermore, the beta activities of the two hemispheres are different in the temporal areas for positive or negative emotions and in the parietal areas for cognitive tasks. Zheng et al. [41] found that EEG patterns for emotion recognition are relatively stable over time and cross-sessions. Particularly, for positive emotions, the lateral temporal lobes have higher beta and gamma activations; for neutral emotions, the parietal and occipital lobes have higher alpha responses; and, for negative emotions, the parietal and occipital lobes have significantly higher delta responses, and the prefrontal lobes have higher gamma responses. Peng et al. [42] proposed an approach to automatically identify important features, and critical frequency bands and channels, in EEG-based emotion recognition. They found that the gamma band, and prefrontal and left/right central channels are important. Results from these studies may be used to select the few most useful EEG channel locations for specific aBCIs, reducing the cost and increasing user-friendliness.

Instead of measuring the neural activities by detecting their electrical signals (as in EEG), fMRI [43] measures the neural activities by detecting changes associated with the brain blood flow, and fNIRS [44] uses near-infrared light to estimate cortical hemodynamic activities associated with the neural activities. fMRI and fNIRS have also found applications in aBCIs, as will be introduced in Section V-F.

D. Public aBCI Datasets

Though it is not easy to record aBCI datasets, there have been more than ten public aBCI datasets in the community, as summarized in Table 2 and sorted according to the year the corresponding paper was published. We also list the number of Google Scholar citations to the papers (as of April 15, 2023) as an indicator of their popularity. The three most popular ones are DEAP [35], MAHNOB-HCI [45], and SEED [46].

The Database for Emotion Analysis using Physiological signals (DEAP) [35] includes EEG and peripheral physiological signals (EOG, EMG, GSR, and so on) of 32 participants, while they were watching 40 1-min-long music video excerpts. 22 of the 32 participants also had frontal face video recorded. Each video excerpt was rated by 14–16 volunteers based on arousal, valence, and dominance, and also by each participant based on arousal, valence, like/dislike, dominance, and familiarity.

MAHNOB-HCI [45] is one of the three databases in the MAHNOB family (laughter, HCI-tagging, and MHI-mimicry). It includes video, audio, eye tracking, and physiological signals (EEG, ECG, RSP, and ST) of 30 participants, while they were watching 20 emotional movie clips. Each participant self-reported his/her ratings of valence, arousal, dominance, and predictability, and also emotional keywords (anger, anxiety, fear, sadness, disgust, neutrality, surprise, amusement, and joy).

The Shanghai Jiao Tong University Emotion EEG dataset (SEED) [46], collected and released by the second author of this tutorial, has been developed into a family of datasets.

1) *SEED:* It includes both EEG (62-channel ESI NeuroScan System) and eye movement (SMI eye-tracking glasses) data of 12 subjects and EEG data only of another three subjects. Data were collected when the

Table 1 EEG Frequency Bands and Emotions [26], [38], [39]

Band	Typical Lobes	Frequency (Hz)	Emotions/States
Delta	Frontal (adults) or posterior (children)	0.5-4	Deep sleep
Theta	Lobes unrelated to task at hand	4-8	Drowsiness, idling
Alpha	Posterior	8-13	Relaxed, reflecting, meditation, elation
Beta	Frontal	13-30	Active thinking, focus, high alert, anxious
Gamma	Somatosensory	30-42	Cognitive processes, e.g., attention and memory
Mu	Somatosensory cortex	8-12	Sadness, sympathy

Table 2 Public aBCI Datasets

Dataset	Year	Number of Subjects	Ages	Stimuli	Modalities	Dimensional States	Discrete States	Number of Citations
MAHNOB-HCI [45]	2012	30	19-40 (mean 26.06)	20 video clips (34.9-117 seconds)	EEG, ECG, RSP, ST, gaze, video, audio	Valence (1-9), arousal (1-9), dominance (1-9), predictability (1-9)	Anger, anxiety, fear, sadness, disgust, neutrality, surprise, amusement, joy	1,304
DEAP [35]	2012	32	19-37 (mean 26.9)	40 music video clips (1 minute)	EEG, EOG, EMG, GSR, RSP, BP, ST	Valence (1-9), arousal (1-9), dominance (1-9), liking (1-9), familiarity (1-9)	None	3,430
SEED [46]	2015	15	Not reported (mean 23.27)	15 film clips (4 minutes)	EEG, EM	None	Positive, negative, neutral	1,163
ASCERTAIN [47]	2016	58	Not reported (mean 30)	36 movie clips (51-127 seconds)	EEG, ECG, GSR, facial activity	Valence (-3-3), arousal (0-6), engagement, liking, familiarity	None	359
DEAMER [48]	2017	23	22-33 (mean 28.3)	18 film clips (65-393 seconds)	EEG, ECG	Valence (1-5), arousal (1-5), dominance (1-5)	Anger, fear, sadness, disgust, calmness, surprise, amusement, happiness, excitement	513
AMIGOS [49]	2018	40	21-40 (mean 28.3)	16 video clips (51-150 seconds)	EEG, ECG, GSR, full body video	Valence (1-9), arousal (1-9), dominance (1-9), familiarity (1-9), liking (1-9)	Anger, fear, sadness, disgust, neutrality, surprise, happiness	363
RCLS [50]	2019	14	21-26 (mean 23.3)	15 video clips	EEG	None	Happy, sad, neutral	64
MPED [51]	2019	23	18-24 (mean 21.46)	28 video clips (2.5-5 minutes)	EEG, ECG, RSP, GSR	Valence, arousal, differential emotion scale	Joy, funny, disgust, anger, fear, sadness, neutrality	148
SEED-IV [52]	2019	15	20-24 (Not reported)	72 film clips (2 minutes)	EEG, EM	Valence, arousal	Happy, sad, fear, neutral	435
HR-EEG4EMO [53]	2020	27	Not reported (mean 35.0)	13 Video clips (40-360 seconds)	EEG, GSR, ECG, RSP, SpO2, pulse rate	Valence	Positive, negative	80
SEED-V [54]	2022	16	19-28 (mean 23.27)	15 film clips (2-4 minutes)	EEG, EM	None	Happy, sad, disgust, fear, neutral	36
SEED-FRA [55]	2022	8	Not reported (mean 22.5)	21 film clips (1-4 minutes)	EEG, EM	None	Positive, negative, neutral	4
SEED-GER [55]	2022	8	Not reported (mean 22.25)	20 film clips (1-4 minutes)	EEG, EM	None	Positive, negative, neutral	4
OVPD [56]	2022	10	23-45 (Not reported)	32 film clips (40-140 seconds), odor	EEG	Valence, arousal	Positive, negative, neutral	3

ECG: Electrocardiogram; EMG: Electromyogram; EOG: electrooculogram; RSP: respiration; ST: skin temperature; GSR: galvanic skin response; EM: eye movement; BP: blood pressure; SpO2: peripheral oxygen saturation.

subjects were watching film clips, carefully selected to elicit different emotions (positive, negative, and neutral).

2) *SEED-IV:* As an evolution of SEED, the number of emotion categories in SEED-IV changes to four: happy, sad, fear, and neutral. EEG and eye movement data are provided.
3) *SEED-V:* As an evolution of SEED-IV, the number of emotion categories in SEED-V increases to five: happy, sad, fear, disgust, and neutral. EEG and eye movement data are provided.
4) *SEED-FRA:* This dataset contains EEG and eye movement data of eight French subjects with positive, negative, and neutral emotions.
5) *SEED-GER:* This dataset contains EEG and eye movement data of eight German subjects with positive, negative, and neutral emotions.
6) *SEED-VIG:* Different from the above five emotion datasets, SEED-VIG targets vigilance estimation. Subjects played a driving game in a virtual driving system, with an enormous screen placed in front of a real car. Their EEG and EOG data were collected, and the vigilance level was labeled with the PERCLOS [57] indicator by an eye tracker.

III. SIGNAL PROCESSING IN aBCIs

EEG signals are very weak (typical magnitude: 5–300 μV) and easily contaminated by artifacts (such as eye blinks and muscle movements) and noise. Thus, it is very important to perform signal processing to increase their signal-to-noise ratio.

Signal processing in aBCIs typically includes sequentially temporal filtering, rereferencing, artifact removal, resampling, and epoching.

A. Temporal Filtering

Not all frequencies in EEG are useful for emotion recognition, e.g., the very low frequencies may be dc drifts, and very high frequencies may be noise. Thus, usually, EEG signals need to be bandpass filtered. A commonly used passband is 4–45 Hz [58]. However, recent research has shown that the delta band (0.5–4 Hz) power may be very useful in characterizing negative emotions [41], and high-pass filtering EEG at 1 Hz was recommended for independent component analysis (ICA) [59]; thus, a better passband choice may be 1–45 Hz.

In addition, notch filtering may be used to remove the 50-/60-Hz powerline interference.

B. Rereferencing

EEG records the voltages with respect to a specific reference. Typical reference electrodes [60] include one mastoid (e.g., TP10), linked mastoids, the vertex electrode (Cz), single or linked earlobes, or the nose tip. Headsets with active electrodes may record EEG reference-free. Rereferencing is usually performed after data recoding and filtering to increase the signal-to-noise ratio; particularly, rereferencing post hoc can remove 40-dB unnecessary noise of active headsets [60].

The most frequently used rereferencing approach is the common average reference [58], which removes the mean of all channels from each individual channel. Special attention should be paid when the original EEG signals were recorded with reference [60]

1) If the data were recorded with reference to the nose tip or ear lobe, then these reference electrodes should be excluded from computing the average reference.
2) If N-channel EEG data were recorded with reference to a particular electrode, e.g., TP10, then the signal of TP10 can be recovered from the N-channel data first, i.e., TP10 $=$ (Sum of N electrode activities)$/(N+1)$. Now, there are $N+1$ electrodes, and their average can be computed and removed from each individual electrode.

C. Artifact Removal

The next step is usually artifact (e.g., eye blinks and muscle movements) removal. Many researchers remove artifacts manually, but semiautomatic approaches, such as ICA [61], blind source separation [62], and principal component analysis (PCA), are also popular. They aim to find some spatial filters to transform the original EEG channels into some (usually fewer) "virtual channels," some of which may be artifacts/noise and, hence, could be removed.

Due to volume conduction effects [63], each EEG channel may measure the compound from multiple underlying primary sources in the brain. ICA is one of the most popular approaches to separate these sources. It identifies multiple independent component filters to produce maximally temporally independent signal sources available in the original data. A certain signal source may be eye blinks and, hence, can be removed.

ICA has two main differences from PCA [64].

1) Each successive PCA component accounts for as much as possible of the remaining activity not accounted for by previous PCA components, so different PCA components may have dramatically different contributions, with the first the maximum (could be more than 50%). ICA components have much more homogeneous contributions, ranging from roughly 5% down to ∼0%, because ICA tries to identify maximally independent activity sources.
2) PCA components of EEG data are spatially or temporally orthogonal, depending on which dimension PCA is applied to. ICA components are maximally temporally independent, but there are no spatial constraints.

Recently, end-to-end deep learning approaches [65] have also been proposed for EEG artifact removal.

D. Resampling

EEG signals are typically recorded at a much higher sampling rate (e.g., 1024 Hz) than the useful frequencies in emotion recognition, so usually downsampling is used to reduce the memory and computational cost. Many studies downsampled EEG data to 128 Hz [58].

E. Epoching

EEG signals are usually recorded continuously for each stimulus, which may last several minutes. Each such piece of EEG data may be viewed as a block, and usually, each block is further partitioned into many overlapping or nonoverlapping shorter (e.g., 10 s) epochs to increase the number of trials in analysis.

F. Signal Processing for fMRI-/fNIRS-Based aBCIs

An fMRI image consists of multiple sequentially sampled slices. Its processing typically involves the following steps [66].

1) *Slice timing correction*, which interpolates the slices so that they can be viewed as being sampled at exactly the same time [67].
2) *Realignment*, which performs motion correction to eliminate the effect of head movements [68].
3) *Coregistration*, which registers low spatial resolution fMRI images to a high-resolution structural MRI image of the same subject [69].
4) *Normalization*, which registers a subject's anatomical structure to a standardized stereotaxic template [70].

Currently, there is no standard fNIRS signal processing procedure. Some studies [71], [72] included the following steps, among others:

1) *artifact removal*, which identifies and removes noisy channels and incorrect trials, and removes/corrects motion artifacts;

Table 3 Representative EEG Features in aBCIs

Category	Features
Time domain	Mean, standard deviation, power, un-normalized and normalized 1st/2nd differences, Hjorth's activity/mobility/complexity, normalized non-stationarity index, fractal dimension, higher order crossings
Frequency domain	Band power derivatives (e.g., mean, minimum, maximum, variance, ratio of mean powers of different bands, differential entropy), differential asymmetry, rational asymmetry, DLAT, DCAU, bispectrum, bicoherence, higher order spectra (e.g., bispectra and bicoherence magnitudes)
Time-frequency domain	Short-time Fourier transform and its spectrograms, discrete wavelet transform, Cohen's class, Zhao-Atlas-Marks transform, empirical mode decomposition
Brain connectivity	Pearson correlation coefficient, phase locking value, phase lag index

2) *filtering*, which uses a finite impulse response band-pass filter to remove both very-low-frequency and high-frequency noises;
3) *epoching*, which partitions the fNIRS signal into short trials.

IV. FEATURE EXTRACTION IN aBCIs

EEG is multichannel time series, so time-domain, frequency-domain, time–frequency-domain, and brain connectivity features [73], [74] could be extracted for aBCIs, as summarized in Table 3.

A. Time-Domain Features

Let $\boldsymbol{x}(t) \in \mathbb{R}^T$ be the time series of a single EEG channel, where T is the number of time samples. Time-domain features could include [73]:

1) *Mean:* $\mu_{\boldsymbol{x}} = (1/T)\sum_{t=1}^{T} \boldsymbol{x}(t)$.
2) *Standard deviation:* $\sigma_{\boldsymbol{x}} = ((1/T)\sum_{t=1}^{T}(\boldsymbol{x}(t) - \mu_{\boldsymbol{x}})^2)^{1/2}$.
3) *Power:* $P_{\boldsymbol{x}} = (1/T)\sum_{t=1}^{T} \boldsymbol{x}^2(t)$.
4) *First difference [9] that approximates the gradient:* $\delta_{\boldsymbol{x}} = (1/T-1)\sum_{t=1}^{T-1} |\boldsymbol{x}(t+1) - \boldsymbol{x}(t)|$.
5) *Normalized first difference [9] or normalized length density [75] that captures self-similarities of the time series:* $\bar{\delta}_{\boldsymbol{x}} = \delta_{\boldsymbol{x}}/\sigma_{\boldsymbol{x}}$.
6) *Second difference [9]:* $\gamma_{\boldsymbol{x}} = (1/T-2)\sum_{t=1}^{T-2} |\boldsymbol{x}(t+2) - \boldsymbol{x}(t)|$.
7) *Normalized second difference [9]:* $\bar{\gamma}_{\boldsymbol{x}} = \gamma_{\boldsymbol{x}}/\sigma_{\boldsymbol{x}}$.
8) *Hjorth's activity [76] that is the variance or mean power of the EEG signal:* $A_{\boldsymbol{x}} = \sigma_{\boldsymbol{x}}^2$.
9) *Hjorth's mobility [76] that may be considered as a mean frequency:* $M_{\boldsymbol{x}} = \sigma_{\dot{\boldsymbol{x}}}/\sigma_{\boldsymbol{x}}$, where $\dot{\boldsymbol{x}}$ is the first derivative of $\boldsymbol{x}$.
10) *Hjorth's complexity [76] that measures more details of the EEG signal with reference to the sine wave:* $C_{\boldsymbol{x}} = M_{\dot{\boldsymbol{x}}}/M_{\boldsymbol{x}}$.
11) *Normalized nonstationarity index (NSI) [77] that uses the variation of the local average over time to represent the signal complexity:* $\boldsymbol{x}(t)$ is first normalized by the standard deviation and then divided into multiple small segments. The mean of each segment is computed, and the NSI is the standard deviation of these means.
12) *Fractal dimension [78] that is also a measure of signal complexity:* First, rewrite $\boldsymbol{x}(t)$ as $\{\boldsymbol{x}(m), \boldsymbol{x}(m+k), \ldots, \boldsymbol{x}(m+k\lfloor(T-m/k)\rfloor)\}$, where k is the time interval, $m \in \{1, \ldots, k\}$ is the initial time, and $\lfloor\cdot\rfloor$ is the floor operation. Then, compute

$$L_m(k) = \frac{\sum_{k=1}^{\lfloor \frac{T-m}{k} \rfloor} |\boldsymbol{x}(m+ik) - \boldsymbol{x}(m+(i-1)k)|}{\frac{T-1}{k^2 \lfloor \frac{T-m}{k} \rfloor}}.$$

The fractal dimension is finally computed as the negative slope of the log-log plot of $(1/k)\sum_{m=1}^{k} L_m(k)$ against k.
13) *Higher order crossings (HOCs) [79] that captures the EEG oscillatory pattern:* Apply k different high-pass filters to a zero-mean time series to obtain k filtered time series, and extract the k HOC features as the number of zero-crossings of them.

The first seven time-domain features are generic, i.e., they can be computed for any time series, not necessarily specific to EEG. Hjorth's three measures were specifically proposed for EEG signal analysis.

B. Frequency-Domain Features

Different EEG frequency bands may reflect different emotions, as shown in Table 1. Thus, frequency-domain features [73] usually include band power derivatives (e.g., mean, minimum, maximum, variance, ratio of mean powers of different bands, and differential entropy (DE) [80]) and higher order spectra (e.g., bispectra and bicoherence magnitudes [81]).

An effective and popular frequency-domain feature in EEG-based emotion recognition is DE [80]

$$\begin{aligned}\mathrm{DE}_{\boldsymbol{x}} &= -\int_{-\infty}^{+\infty} \frac{e^{-\frac{(x-\mu_{\boldsymbol{x}})^2}{2\sigma_{\boldsymbol{x}}^2}}}{\sqrt{2\pi\sigma_{\boldsymbol{x}}^2}} \log\left(\frac{1}{\sqrt{2\pi\sigma_{\boldsymbol{x}}^2}} e^{-\frac{(x-\mu_{\boldsymbol{x}})^2}{2\sigma_{\boldsymbol{x}}^2}}\right) dx \\ &= \frac{1}{2}\log\left(2\pi e\sigma_{\boldsymbol{x}}^2\right).\end{aligned}$$

For a fixed-length EEG sequence, DE is equivalent to the logarithmic energy spectrum in a certain frequency band [82].

Differential asymmetry (DASM) and rational asymmetry (RASM), which are the difference and ratio between the DEs of a pair of hemispherically symmetric electrodes (e.g., O1 and O2 in Fig. 5, denoted as $\boldsymbol{x}_{\text{left}}$ and $\boldsymbol{x}_{\text{right}}$), respectively, can further be extracted to describe the hemispheric asymmetry [80]

$$\begin{aligned}\mathrm{DASM} &= \mathrm{DE}_{\boldsymbol{x}_{\text{left}}} - \mathrm{DE}_{\boldsymbol{x}_{\text{right}}} \\ \mathrm{RASM} &= \frac{\mathrm{DE}_{\boldsymbol{x}_{\text{left}}}}{\mathrm{DE}_{\boldsymbol{x}_{\text{right}}}}.\end{aligned}$$

Similar differential spectral asymmetry features, DLAT and DCAU, were also proposed in [83]. DLAT consists of the differential spectral band powers (delta, theta,

alpha, beta, and gamma) for 12 left-right electrode pairs, e.g., Fp1-Fp2 and F7-F8. The latter consists of those for 12 fronto-posterior electrode pairs, e.g., Fp1-O1 and F7-P7.

The bispectrum Bis is the Fourier transform of the third-order moment of $\boldsymbol{x}(t)$, i.e., [73], [81]

$$\mathrm{Bis}(f_1, f_2) = E\left[\mathrm{FT}(f_1) \cdot \mathrm{FT}(f_2) \cdot \mathrm{FT}^*(f_1 + f_2)\right]$$

where E is expectation, FT is the Fourier transform of $\boldsymbol{x}(t)$, and * is the complex conjugate.

Bicoherence Bic is the normalized Bis [73], [81]

$$\mathrm{Bic}(f_1, f_2) = \frac{\mathrm{Bis}(f_1, f_2)}{\sqrt{P(f_1) \cdot P(f_2) \cdot P(f_1 + f_2)}}$$

where $P(f) = E[\mathrm{FT}(f) \cdot \mathrm{FT}^*(f)]$ is the power spectrum.

Several other entropy features, e.g., approximate entropy [84], sample entropy [84], permutation entropy [85], and dispersion entropy [86], have also been proposed and used in EEG-based emotion recognition [87].

Giannakakis et al. [88] gave a review on biosignal-based psychological stress detection and concluded that EEG alpha asymmetry index (e.g., the natural logarithm of the Alpha power of F3 minus that of F4) is consistently reduced under stress.

C. Time–Frequency-Domain Features

Time–frequency-domain features are usually 2-D spectral representations of EEG signals in simultaneously time and frequency domains [89], including short-time Fourier transform (STFT), spectrograms computed from STFT [89], discrete wavelet transform [90], Cohen's class [91], Zhao–Atlas–Marks (ZAM) transform [92], empirical mode decomposition (also known as Hilbert–Huang spectrum (HHS) [93], [94]), and so on.

Hadjidimitriou and Hadjileontiadis [89] compared STFT, ZAM, and HHS features in music like/dislike classification and found that, generally, ZAM features performed the best due to their high resolution in both time and frequency domains.

D. Brain Connectivity

Connectivities between different brain regions (electrodes) have also been used as features in emotion recognition. Frequently used brain connectivity measures [95] are the Pearson correlation coefficient (PCC), phase-locking value (PLV) [96], and phase lag index (PLI) [97].

The PCC measures the linear correlation between two time series $\boldsymbol{x}(t)$ and $\boldsymbol{y}(t)$

$$\mathrm{PCC}_{\boldsymbol{x},\boldsymbol{y}} = \frac{\mathrm{cov}(\boldsymbol{x}, \boldsymbol{y})}{\sigma_{\boldsymbol{x}} \sigma_{\boldsymbol{y}}}$$

where $\mathrm{cov}(\boldsymbol{x}, \boldsymbol{y})$ is the covariance. PCC has a range of $[-1, 1]$, and a PCC of zero means that there is no linear relationship between $\boldsymbol{x}(t)$ and $\boldsymbol{y}(t)$.

Define $\boldsymbol{z}(t) = \boldsymbol{x}(t) + j\tilde{\boldsymbol{x}}(t)$, where $j = \sqrt{-1}$, and

$$\tilde{\boldsymbol{x}}(t) = \frac{\mathrm{PV}}{\pi} \int_{-\infty}^{\infty} \frac{\boldsymbol{x}(\tau)}{t - \tau} d\tau$$

is the Hilbert transform of $\boldsymbol{x}(t)$, in which PV is the Cauchy principal value. The instantaneous phase $\phi(t)$ of $\boldsymbol{x}(t)$ is then

$$\phi(t) = \arctan \frac{\tilde{\boldsymbol{x}}(t)}{\boldsymbol{x}(t)}.$$

The PLV [96] computes the phase synchronization between Channels i and k, by taking the absolute average of phase differences over temporal windows

$$\mathrm{PLV}(i, k) = \left| \frac{1}{T} \sum_{t=1}^{T} e^{j(\phi_i(t) - \phi_k(t))} \right|.$$

The PLI [97] is another way to compute the phase synchronization between channels i and k

$$\mathrm{PLI}(i, k) = \left| \frac{1}{T} \sum_{t=1}^{T} \mathrm{sign}\left(\phi_i(t) - \phi_k(t)\right) \right|.$$

Both PLV and PLI take values in $[0, 1]$. A larger value indicates better phase locking, and a value of zero means of two channels are independent.

Moon et al. [95] performed binary arousal classification on DEAP and found that the PCC and PLV features always outperformed power spectrum density (PSD) features when fed into convolutional neural networks, and PLV always outperformed PLI.

E. Feature Combinations

Different feature extraction approaches could also be assembled into a pipeline to extract new features.

A frequently used approach is to extract more features from different frequency bands. Hadjidimitriou and Hadjileontiadis [89] computed the spectrograms of STFT, ZAM transform, and Hilbert–Huang spectrum in both beta (13–30 Hz) and gamma (31–49 Hz) bands and then concatenated them as features for music appraisal responses (like and dislike) classification. Zheng et al. [41] used PSD, DE, DASM, RASM, and so on in five different frequency bands for emotion classification on DEAP and SEED.

Another idea is to extract more features from different intrinsic mode functions in empirical mode decomposition. Liu et al. [98] first performed empirical mode decomposition of the original EEG signals to obtain five intrinsic mode functions and then computed the DE for each intrinsic mode function and each channel. The dynamic DE features

were then used by a convolutional neural network for emotion classification.

Kroupi et al. [75] extracted power ratio features from theta, alpha, low beta (13–16 Hz), middle beta (17–20 Hz), high beta (21–29 Hz), and low gamma (30-47 Hz) bands, by dividing a subject-specific baseline power from the trial powers. Additional features included the Wasserstein distance between trial and baseline powers, and the normalized length density index.

F. Feature Extraction for fMRI-/fNIRS-Based aBCIs

Functional connectivities between brain regions of interest (ROIs) are common fMRI features in aBCIs [99], [100]. The ROIs could be defined according to the atlas of automated anatomical labeling [101], dense individualized and common connectivity-based cortical landmarks (DICCCOLs) [102], and so on. Then, measures such as small-world parameters [103], network efficiency [104], and nodal centrality metrics [105] could be computed.

For fNIRS feature extraction [106], the raw fNIRS light intensities could be converted to relative changes in hemodynamic responses in terms of oxy-hemoglobin (Hbo) and deoxy-hemoglobin (Hbr), and then, Hbo + Hbr and Hbo-Hbr, which estimate the total blood volume and the oxygenation change, can be calculated for each optode. Finally, their statistics such as mean, median, standard deviation, maximum, minimum, and maximum–minimum could be extracted as features.

V. EMOTION RECOGNITION IN aBCIs

Once the features are extracted, traditional machine learning algorithms, e.g., k-nearest neighbors [107], decision tree [107], and support vector machine (SVM) [108], can be used for emotion recognition. When deep learning [109] is used, feature extraction and classification/regression can be integrated into a single end-to-end neural network, so manual feature extraction may not be necessary.

A. Within-Subject Emotion Recognition

Many aBCI studies performed within-subject emotion recognition, where each subject is considered individually. Both traditional machine learning approaches [110] and deep learning have been considered.

For example, Huang et al. [15] performed within-subject EEG-based binary (positive/negative) emotion classification for both healthy subjects and disorder-of-consciousness patients, using manually extracted PSD features and an SVM classifier. The ten healthy subjects achieved on average over 90% classification accuracy, and some disorder-of-consciousness patients also achieved about 70% accuracy. Liu et al. [111] proposed a 3-D convolution attention neural network for both within- and cross-subject EEG emotion classifications on SEED. In within-subject classification, it outperformed a deep convolutional neural network using electrode-frequency distribution map features [112], a deep canonical correlation analysis model fusing EEG functional connectivity network features and eye movement features [113], and a spiking neural network model [114].

We should note that, for within-subject emotion recognition, it is very important to perform cross-block data partition and evaluations.

For example, SEED includes 15 4-min film clips for each subject. Each 4-min EEG data recording for a film clip can be viewed as a block, and each block can be partitioned into multiple shorter nonoverlapping trials (e.g., 10 s) to increase the number of training and test samples. Thus, each block consists of 24 trials with the same emotion label, and there are a total of $24 \times 15 = 360$ trials.

For within-subject emotion recognition, each subject is considered individually. It is very important that the training and test sets should come from different blocks, e.g., Blocks 1–12 for training and Blocks 13–15 for test. If we mix the 360 trials altogether and randomly select 80% of them for training and the remaining 20% for testing, then there is a block-design pitfall [115]: "the block design leads to the classification of arbitrary brain states based on block-level temporal correlations that are known to exist in all EEG data, rather than stimulus-related activity. Because every trial in their test sets comes from the same block as many trials in the corresponding training sets, their block design, thus, leads to classifying arbitrary temporal artifacts of the data instead of a stimulus-related activity."

The block-design pitfall becomes more significant if each 4-min EEG block is partitioned into multiple overlapping trials. For example, if the [0, 10] second trial in a certain block is used in training, and the subsequent [5], [15] second trial from the same block is used in the test, then there is data leakage since part of the test data have been seen in training, and hence, the test results will be overoptimistic.

B. Transfer Learning for Cross-Subject/ Cross-Session Emotion Recognition

A machine learning model may work well when there are adequate training data, and the training and test data have the same distribution. Unfortunately, these two assumptions are not always satisfied in aBCIs: 1) for fast calibration to improve system utility and user-friendliness, it is desirable to collect as few calibration trials from a new subject as possible, i.e., the subject-specific training data is usually not enough and 2) due to large individual differences (data distributions from different subjects are usually significantly different), generally, it is not feasible to use data from existing subjects directly for the calibration of a new subject.

Transfer learning [116] has been widely used in BCIs [117], including aBCIs, to reduce the subject-specific calibration effort. Transfer learning uses data or knowledge from some source domains (existing subjects) to facilitate the model training in a target domain (a new subject).

To reduce the domain discrepancy and, hence, overcome negative transfer [118], transfer learning may weigh the source domain samples so that their distribution is more similar to that of the target domain (instance transfer) or perform feature transformations so that the feature distributions of the source and target domains are more similar in the new feature space (feature transfer) or use the source models to regularize the target model (parameter transfer) and so on.

For instance transfer, Zhang et al. [119] proposed individual similarity-guided transfer learning for EEG-based emotion recognition. They used first maximum mean discrepancy (MMD) to quantify the similarities between the source subjects and the target subject, then TrAdaBoost to further weight the trials from the top few most similar source subjects to make the axillary data distribution more resemble the target distribution, and, finally, an SVM for classification. Lin [120] first used the Riemannian distances of MESH features (concatenation of DLAT, DCAU, and PSD features) [83] between multiple source sessions and the target session to select the most similar few source sessions and then augmented their data with the target session data for cross-session transfer. Particularly, matrix factorization of robust PCA was further used to reweight the samples for instance transfer.

For feature transfer, Zheng et al. [121] demonstrated the promising performance of two classical feature dimensionality reduction approaches, transfer component analysis [122], and kernel principal analysis [123] in EEG-based emotion classification on SEED. Both aim to learn a set of common transferrable components between the source and target domains in a latent feature space. Chai et al. [124] proposed adaptive subspace feature matching, which uses first PCA in the source and target domains, respectively, to map the DE features into lower dimensional subspaces, then a linear transformation matrix to match their marginal distributions, and, finally, conditional distribution adaptation to further reduce the distribution discrepancy.

EEG data alignment approaches, e.g., Riemannian alignment [125] and Euclidean alignment [126], may also be used to transform the EEG data from different subjects so that their distributions are more consistent (and hence to facilitate transfer learning); thus, they may also be viewed as feature transfer approaches. For example, Wang et al. [127] demonstrated the effectiveness of the Riemannian Alignment-Minimum Distance to Riemannian Mean (RA-MDRM) [125] on DEAP, and Jiang et al. [128] demonstrated the effectiveness of Euclidean alignment on both DEAP and SEED.

For parameter transfer, Zheng and Lu [129] used source domain data to train multiple SVM classifiers, one for each domain, and then learned a regression function to describe the relationship between the feature distribution and SVM parameters. The parameters of the target domain SVM classifier were then computed by applying such a function to the unlabeled target data.

Li et al. [130] reviewed transfer learning for EEG-based emotion recognition and observed that the research interest is gradually shifting from instance transfer, to feature transfer, and then to parameter transfer (their Table 2 summarizes about 20 representative transfer learning approaches in aBCIs). So far, feature transfer has the most investigations. They also gave a summary of the performance of some representative transfer learning approaches, in cross-session, cross-subject, and cross-database transfers. The state-of-the-art cross-subject transfer learning classification accuracies on SEED are around 90% for three-class valence classification [112], [131].

C. Deep Transfer Learning

Deep learning [132], which has achieved great success in many other domains, has also been gaining popularity in aBCIs. In deep learning [109], feature extraction and classification/regression are integrated into a single neural network and simultaneously optimized.

Deep learning-based transfer learning, or deep transfer learning, can be achieved in different ways. The most popular and straightforward approach [112] is parameter transfer, i.e., to train a deep learning model using data from multiple auxiliary subjects and then adapt it to the new subject by fixing the first few feature extraction layers and then using the subject-specific data to fine-tune the last few classification layers. Another idea is to use adversarial learning to bring the data distributions of the auxiliary and new subjects closer. For example, Luo et al. [133] proposed the Wasserstein generative adversarial network domain adaptation to achieve an 87% cross-subject emotion classification accuracy on SEED. It uses first pretraining to map source and target domains to common latent feature space and then adversarial training to bring the source and target domain latent features together.

D. Multimodal Learning

Multimodal signals, e.g., EEG, ECG, eye movement, and facial expressions, may be used together for more reliable emotion recognition. An important question is how to effectively fuse the information from different modalities.

Generally, there are two popular fusion strategies in multimodal emotion recognition.

1) Feature-level fusion, where features of each modality are extracted individually and independently, and then concatenated into a single larger feature vector for classification or regression. For example, Wu et al. [108] concatenated features from four physiology signals (EEG, ECG, skin conductance level, and respiration) and then used an SVM for subject-dependent classification of three arousal levels, reaching an average accuracy of 96.5% on 18 subjects. Cai et al. [107] performed feature-level fusion for multimodal depression recognition. They collected EEG signals, while the subjects were listening to audio with different emotions (neutral, negative, and

positive), each emotion being viewed as a modality. For each subject, EEG features from each modality were computed, and features from the three modalities were linearly combined to form a new feature vector, which was used to classify if the subject had depression or not.

2) Decision-level fusion, which builds a classifier for each modality and then aggregates their results. Usually, the outputs of each classifier are the classification confidence of different classes, and there are different approaches to aggregate this confidence [134], e.g., (weighted) summation, product, Dempster–Shafer, and Bayesian belief integration. For example, Huang et al. [135] used neural networks to classify four emotions (happiness, neutral, sadness, and fear) from facial expressions, and two SVMs to classify these four emotions and three intensities (strong, ordinary, and weak) from EEG, respectively. Summation and product decision-level fusion approaches were then used for multimodal emotion detection, both outperforming single-modal detection.

There is no universal conclusion on which fusion approach is better. Zheng et al. [136] compared both fusion strategies in EEG and eye-tracking data-based emotion classification on SEED and found that, on average, feature-level fusion outperformed two decision-level fusion approaches (73.59% versus 72.98% and 68.90%). Soleymani et al. [137] used EEG, pupil diameter, eye blinks, and gaze distance for subject-independent classification of three arousal levels (calm, medium aroused, and activated) and three valence classes (unpleasant, neutral, and pleasant). They found that decision-level fusion outperformed feature-level fusion, reaching 68.5% and 76.4% average classification accuracies on arousal and valence, respectively, on 24 subjects.

E. Cross-Modal Learning

In real-world applications of aBCIs, maybe not all input signals used in training are available in the test, e.g., both EEG and eye movement signals are used in training, whereas only eye movement signals are available in the test. In this case, using all available modalities in training may still be more beneficial than using only one of them.

Zheng et al. [138] considered modality deficiency in heterogeneous transfer learning, i.e., the source subjects have both EEG and eye movement signals, whereas the target subject has only eye movement signals. They showed that with only eye tracking data for the target subject, TL can still make use of the discriminative information in EEG from the source subjects, achieving comparable performance with the model based on EEG data in emotion recognition. This greatly extends the application scenarios of aBCIs, as eye trackers may be easier to wear, and eye tracking data may be less subjective to body movement artifacts.

Yan et al. [139] investigated the same problem using a different approach. They first used EEG and eye movement features to train a multimodal fusion network and an emotion classifier and then trained a conditional generative adversarial network to learn the relationship between eye movements and the multimodal features. In the test phase, eye movement features were used to regress multimodal features for emotion classification.

Eye movements should not play a role in some BCI paradigms, e.g., motor imagery; thus, they are called artifacts there and should be removed. However, multiple studies [137], [138], [139] verified that they could be very useful in aBCIs. For example, Soleymani et al. [137] showed that eye gaze features outperformed EEG in video-elicited emotion classification, and their decision-level fusion performed the best. This should not diminish the usefulness of EEG in aBCIs, as, in real-world applications, vision is not the only input to elicit emotions; other emotional inputs, such as sound and smell, may be reflected by EEG but not eye movements.

F. fMRI-/fNIRS-Based Emotion Recognition

In addition to EEG, fMRI and fNIRS have also been used in emotion recognition.

Han et al. [100] combined fMRI-derived features (functional connectivities between ROIs, computed by the wavelet transform coherence) and low-level audio–visual features (lighting key, color energy, visual excitement, Mel-frequency cepstral coefficients, and so on) for binary video arousal classification (low and high), and showed that fMRI-derived features can increase the subject-dependent classification accuracy by more than 10%. fMRI-derived features themselves achieved over 92% cross-subject classification accuracies on three subjects.

Wang et al. [140] studied intersession instability in fNIRS-based emotion recognition and found a 22.2% average deterioration of binary emotion classification (negative and neutral) accuracy between two sessions with three-week apart. As the change of the distributions of fNIRS features may be the cause of the performance decline, they proposed a feature selection approach that considers both the feature separability and their stability over time, which gave a 5% accuracy improvement in cross-session classification.

Sun et al. [106] showed that using EEG and fNIRS simultaneously for positive/negative arousal classification outperformed every single modality. The logarithmic PSD for theta, slow alpha (8–10 Hz), alpha, and beta bands was extracted from each electrode as EEG features. The mean, median, standard deviation, maximum, minimum, and maximum–minimum of Hbo + Hbr and Hbo-Hbr from each optode were extracted as fNIRS features. In addition, brain activity asymmetry features, i.e., the difference between the spectral powers of symmetrical EEG electrode pairs on the two hemispheres, were also extracted.

VI. BRAIN STIMULATION

Brain stimulation in aBCI is used to achieve emotion regulation [141], which "refers broadly to implementation of a conscious or nonconscious goal to start, stop, or otherwise modulate the trajectory of an emotion." Proper emotion regulation is important in mental and physical health, and social interactions [142].

Multiple EEG-based emotion biomarkers have been proposed in the literature. For example, Hardt and Kamiya [143] found that, for high anxiety subjects, increasing EEG Alpha activity reduced anxiety and vice versa. Thus, they suggested that long-term alpha feedback training (>5 h) may be useful in anxiety therapy. The asymmetry in frontal alpha power also indicates different emotions [144]: greater right-lobe alpha activity than left-lobe activity is associated with negative emotions and vice versa. These findings have been used to guide the design of EEG-based neurofeedback training to regulate [142] "single-frequency band EEG activity in specific brain regions or EEG power differences between hemispheres." Huang et al. [142] further developed an EEG-based BCI for emotion regulation, which uses video clips to regulate the user's emotion directly to a certain state (positive, neutral, and negative), instead of regulating the activity of a certain EEG frequency band.

Similar noninvasive emotion regulation studies have also been performed using fMRI [145] and fNIRS [146]. However, instead of regulating the activity of a certain EEG frequency band, they regulate the activity of a certain ROI, e.g., amygdala or dorsolateral prefrontal cortex.

Brain stimulation using electroconvulsive therapy (ECT), transcranial magnetic stimulation (TMS), vagal nerve stimulation (VNS), and deep brain stimulation (DBS) have also been used in treatment-resistant depression (TRD) therapies. Cusin and Dougherty [147] summarized their efficacy, contraindications, and side effects: "ECT is widely available and its effects are relatively rapid in severe TRD, but its cognitive adverse effects may be cumbersome. TMS is safe and well tolerated, and it has been approved by FDA for adults who have failed to respond to one antidepressant, but its use in TRD is still controversial as it is not supported by rigorous double-blind randomized clinical trials. The options requiring a surgical approach are VNS and DBS. VNS has been FDA-approved for TRD; however, it is not indicated for the management of acute illness. DBS for TRD is still an experimental area of investigation, and double-blind clinical trials are underway."

VII. aBCI APPLICATIONS

aBCIs have found applications in education [148], entertainment [149], healthcare [15], and so on. Some representative ones are introduced next.

A. Cognitive Workload Recognition

Cognitive workload may be defined as [150] "the relation between the function relating the mental resources demanded by a task and those resources available to be supplied by the human." Maintaining an appropriate workload helps improve the operator's safety and efficiency. For example, using a Virtual Reality Stroop Task with three difficulty levels and the user's reaction time as the performance measure, Wu et al. [108] empirically verified the Yerkes–Dodson law [151], which states that the performance in mental tasks is a nonmonotonic function of arousal (stress or workload): as arousal increases from low to high, the performance first increases and then decreases.

There may be associations between workload and EEG frequency band power. For example, the increasing workload may lead to alpha band power decrease and theta band power increase [152], [153]. As a result, EEG-based cognitive workload recognition has been used in many different working environments [154], e.g., education [148], air traffic control [155], and autism intervention [156]. Zhou et al. [154] presented a comprehensive review on EEG-based cognitive workload recognition, focusing on machine learning approaches. Both traditional machine learning and deep learning approaches have been extensively used.

B. Fatigue Estimation

Fatigue (drowsiness) is an important contributor to many accidents, particularly traffic accidents. The U.S. National Highway Traffic Safety Administration [157] estimated that, in 2017, drowsy driving resulted in 91 000 police-reported crashes, 50 000 injuries, and nearly 800 deaths. These numbers may be underestimated.

Different strategies, e.g., computer vision-based [158] and driving behavior-based [159], have been used for driver fatigue estimation. EEG-based driver fatigue (drowsiness) estimation, which is less dependent on overt behavior and less susceptible to deception [26], belongs to the latter. Another advantage of EEG-based driver fatigue estimation is that fatigue may be detected from EEG signals earlier than from other modalities like facial expressions, as fatigue originates deep in the brain.

Many different approaches, particularly transfer learning, have been used in EEG-based driver drowsiness estimation [159], [160], [161]. Commercial products, e.g., SmartCap,[1] have also been developed.

C. Depression Diagnosis and Treatment

As indicated by the World Health Organization [162], "depression is a common mental disorder. Globally, it is estimated that 5% of adults suffer from depression. Depression is a leading cause of disability worldwide and is a major contributor to the overall global burden of disease."

Many studies have investigated the use of aBCIs in depression diagnosis, and multiple EEG-based biomarkers were proposed. For example, Allen et al. [163] found that

[1] https://www.smartcaptech.com

prefrontal cortex EEG Alpha asymmetry may be a good indicator of depression. Putnam and McSweeney [164] further found that specific depression symptoms are uniquely associated with prefrontal cortex EEG alpha activity patterns: lower bilateral prefrontal cortex alpha activity for higher levels of rumination and lower right bilateral prefrontal cortex alpha activity for higher levels of self-esteem. Li et al. [165] found that major depression disorder patients have lower N2 amplitudes for all stimuli and reduced anterior cingulate cortex activation for incongruent stimuli. de Aguiar Neto and Rosa [166] gave a review on EEG-based depression biomarkers.

aBCIs have also been extensively used in TRD therapies [147]. One of the latest progress is DBS [167], which implants electrodes within certain areas of the brain to generate electrical impulses to regulate emotion. Using multisite intracranial electrodes implanted in a severely depressed patient, Scangos et al. [168] found "an elaborate repertoire of distinctive emotional responses that were rapid in onset, reproducible, and context and state-dependent" to focal electrical neuromodulation. Rao et al. [169] showed that lateral orbitofrontal cortex stimulation-induced neural features associated with positive mood states and, hence, improved mood state in depression subjects. These pilot studies provided proof of concept for personalized and effective DBS-based treatment of emotion disorders, e.g., severe depression.

VIII. CHALLENGES AND OPPORTUNITIES IN aBCIs

Though we have witnessed rapid progress in aBCI research and applications in the last few decades, multiple challenges still need to be overcome before their broad real-world applications.

A. Brain Signal Acquisition

Common brain signals used in aBCIs include EEG, fMRI, and fNIRS. The latter two require more expensive equipment to acquire, so EEG is currently the most popular aBCI input signal.

There are three types of EEG electrodes: gel-based, water-based, and dry.

Gel-based electrodes use conductive gel to increase the conductivity between the scalp and the electrodes, and hence, the EEG signal quality is usually much better than that of dry electrodes. However, gel injection is time-consuming and user-unfriendly, which may hinder the acceptance of gel-based EEG electrode-based aBCIs to consumers.

Dry electrodes, which do not need conductive gel, are much more convenient to use. Unfortunately, their signal quality still needs improvements [170]. For broad real-world applications, it is very important to develop cheap, convenient, and high-fidelity brain signal acquisition devices.

Water-based electrodes, or semidry electrodes, use tap/saline water or slow-releasing electrolyte liquid to increase the conductivity between the scalp and the electrodes. They seem to be a good compromise between gel-based electrodes and dry electrodes in terms of signal quality and convenience.

B. Emotion Labeling

Unlike videos or music, whose emotions can be labeled by human evaluators directly, it is almost impossible to directly label the emotions of EEG trials. Thus, many aBCI studies used videos or music to elicit emotions and assumed that the subject's EEG has the same emotion label as the stimulating video or music.

For example, a "happy" movie clip rated by multiple evaluators is supposed to elicit a happy emotion from the subject. However, there are several limitations of this approach: 1) because of individual differences, the subject may not feel happy when watching the movie; 2) even though the subject may feel happy, the activation level may be too low to be reflected in his/her EEG signals; and 3) the subject may feel happy for a short duration of the movie, but it is difficult to know which part it is, so it is usually assumed that the subject has a happy emotion during the entire duration of the movie. Because of these reasons, the emotion label for EEG signals may not be accurate.

In addition, people may exhibit multiple emotions simultaneously, e.g., a graduate may feel both happy and sad at the graduation ceremony, and a viewer may feel both sad and angry when seeing a good person killed in a war movie. Unfortunately, currently, most aBCI experiments assign only one emotion label or rating to each movie/music, which may be too simplified.

Thus, more accurate and realistic emotion labeling approaches are needed in aBCIs.

C. Diversity and Size of aBCI Datasets

A closer look at the datasets in Table 2 reveals at least two limitations.

1) The dataset size is very small: the number of subjects ranges from 8 to 58 (most below 30), and the number of stimuli ranges from 13 to 40. Huge datasets in other application domains have greatly boosted their breakthroughs, e.g., ImageNet [171] (more than 14 million images and 20 000 categories) for deep learning in image recognition and more than 680 billion tokens for Generative Pretrained Transformer 3 (GPT-3) [172] in natural language processing. It is expected that larger aBCI datasets will also facilitate more rapid progress of aBCIs.
2) The demography of subjects is not diverse enough: the mean age is between 21 and 35, so children, teenagers, and the elderly are not adequately represented. However, these underrepresented groups are also huge markets for aBCI technologies. For example, the U.S. Centers for Disease Control and Prevention (CDC) estimates that [173], between 2016 and 2019, for children and teenagers aged 3–17 years,

9.4% (approximately 5.8 million) had anxiety, and 4.4% (approximately 2.7 million) had depression. The World Health Organization estimates that 5.7% of adults older than 60 have depression. These large populations should not be overlooked. Due to large individual differences and the subtle nature of emotions, models and strategies developed from datasets of young adults may not be directly applicable to these groups, and dedicated datasets and models should be created for them.

D. Comparison of Different Approaches

New machine learning algorithms are constantly proposed for aBCIs, and their effectiveness is demonstrated in the corresponding publications. Unfortunately, it is challenging to directly compare different algorithms due to the following reasons.

1) Different datasets are used, e.g., researchers may collect their own datasets for performance evaluation. It is desirable to publicize these datasets so that further comparisons can be made, or, if there are restrictions to release the self-collected datasets, then experimental results on some public datasets should also be reported.
2) Different experimental settings, e.g., different splittings of blocks into trials and different partitions of training/validation/test sets. It is recommended to introduce these details as much as possible in the publications.
3) Tricks in algorithm design and optimization, e.g., the structure of the neural network, setting of hyperparameters, and the number of training epochs. It is recommended to share the code with the publications or at least specify these details as much as possible.

E. Negative Transfer in Emotion Recognition

Transfer learning is now prevailing in cross-subject/cross-session calibration of emotion recognition algorithms in aBCIs. However, transfer learning may not guarantee improved performance, i.e., negative transfer [118] could occur.

Zhang et al. [118] pointed out four possible reasons for the negative transfer.

1) Large domain divergence, e.g., negative transfer in emotion recognition may occur when the source and target subjects have significantly different cultural backgrounds.
2) Poor source data quality, e.g., the emotion recognition accuracy of the source subject is too low to be useful in helping the target subject.
3) Poor target data quality, e.g., EEG data from the target subject contain too many artifacts/noise, or the EEG electrodes may be placed at scalp locations that are not responsible for emotions.
4) Inappropriate transfer learning algorithm. Each transfer learning algorithm has its assumptions and specific application scenarios. Choosing an inappropriate one may result in a negative transfer. For example, transfer component analysis [122], a classic transfer learning algorithm, assumes that the source and target domains have the same conditional probability distribution, but different marginal distributions, so it focuses on reducing the latter. It may result in a negative transfer if the conditional distributions are significantly different.

There are also different strategies to mitigate or avoid negative transfer [118], which have not been extensively investigated in aBCIs yet.

1) domain similarity estimation, which is particularly useful in selecting the most similar source domains from multiple ones, i.e., to reduce the domain divergence;
2) safe transfer, which includes deliberately designed algorithms that can avoid negative transfer with theoretical guarantees, regardless of how the source and target subjects are different from each other;
3) negative transfer mitigation, which alleviates negative transfer using data/model transferability enhancements, training process enhancements, and/or target prediction enhancements.

F. Privacy-Preserving aBCIs

Many aBCI studies used transfer learning to facilitate the calibration, making use of EEG data from the source subjects. In addition to emotions, EEG signals also contain other private information [174], e.g., user identity, health status, and psychological state, which may be easily revealed. For example, Kong et al. [175] performed EEG-based user identification on SEED (and three other EEG datasets from different BCI paradigms), achieving over 99% accuracy using only seconds of EEG data.

As a result, user privacy protection in BCIs has become very important [176], [177]. Several recent laws and regulations, e.g., the European General Data Protection Regulation[2] (GDPR; effective since May 25, 2018) and the China Personal Information Protection Law (effective since January 11, 2021), also enforce strict user privacy protection.

Xia et al. [174] summarized three different strategies to implement privacy-preserving BCIs.

1) Cryptography, which includes homomorphic encryption, secure multiparty computation, and secure processors. For example, Agarwal et al. [178] used secure multiparty computation for user privacy protection in EEG-based driver drowsiness estimation. At a reasonable computational cost, they obtained identical results as in the unencrypted case.
2) Perturbation, which transforms or adds noise to the original EEG data while maintaining their utility for

[2]https://gdpr-info.eu/

emotion recognition. It can be implemented through differential privacy or data reconstruction.

3) Machine learning-aided systems, which may be used to [174] "help people better understand privacy policies and inform them about the privacy risks when making privacy decisions."

Recently, Zhang et al. [179] proposed unsupervised multisource decentralized transfer for offline privacy-preserving EEG classification, which implements transfer learning using the source model parameters or predictions, instead of the source data. Experiments on SEED demonstrated that it can achieve simultaneously privacy protection and higher classification accuracy.

Nevertheless, privacy protection of aBCIs has not received enough attention compared with accurate emotion recognition in aBCIs.

G. Secure aBCIs

Recent research found that many machine learning models, including both traditional machine learning and deep learning, are vulnerable to adversarial attacks [180], where deliberately designed tiny perturbations, which may be too small to be noticed by human eyes or detected by computer algorithms, are used to fool a machine learning algorithm.

Both classification and regression models in EEG-based BCIs are subject to adversarial attacks [181], [182], [183], [184], [185]. For example, Meng et al. [186] proposed two adversarial attack approaches for EEG-based regression problems, which can generate small perturbations to change the estimated driver drowsiness level by a predetermined amount, at nearly 100% success rate.

Adversarial attacks on BCIs could lead to serious security and safety problems, as pointed out by a recent report by the RAND Corporation [187]: "hacking BCI capabilities could theoretically provide adversaries with direct pathways into the emotional and cognitive centers of operators' brains to sow confusion or emotional distress. In the extreme, adversary hacking into BCI devices that influence the motor cortex of human operators could theoretically send false directions or elicit unintended actions, such as friendly fire."

Though very important, there has not been research on adversarial defenses for aBCIs. We [188] performed a systematic review on adversarial attacks and defenses in physiological computing, including BCIs, and pointed out several potential adversarial defense strategies:

1) data modification, which improves the adversarial robustness by modifying the training data, e.g., through adversarial training [189], or the test data, e.g., through data compression [190] or randomization [191];
2) model modification, which improves the adversarial robustness by modifying the target model directly, e.g., through regularization [192] and defensive distillation [193];
3) auxiliary tools, which improve the adversarial robustness by using auxiliary machine learning modules, e.g., adversarial detection [194].

Their effectiveness has yet to be validated in aBCIs.

IX. CONCLUSION

Affects, including moods and emotions, are pervasive in our everyday life and are essential in human cognition, communication, and decision-making. An aBCI monitors and/or regulates the emotional state of the brain, which can be used in education, entertainment, healthcare, and so on. This tutorial on aBCIs introduces first the basic concepts of BCIs and then, in detail, the individual components in a closed-loop aBCI system, including signal acquisition, signal processing, feature extraction, emotion recognition, and brain stimulation. It also describes three representative applications of aBCIs, i.e., cognitive workload recognition, fatigue estimation, and depression diagnosis and treatment. Finally, several challenges and opportunities in aBCI research and applications, including brain signal acquisition, emotion labeling, diversity and size of aBCI datasets, algorithm comparison, negative transfer in emotion recognition, and privacy protection and security of aBCIs, are pointed out.

To the best of our knowledge, this is the most comprehensive and up-to-date aBCI tutorial in the literature. ■.

REFERENCES

[1] J. S. Lerner, Y. Li, P. Valdesolo, and K. S. Kassam, "Emotion and decision making," *Annu. Rev. Psychol.*, vol. 66, no. 1, pp. 799–823, 2015.

[2] M. Minsky, *The Society of Mind*. New York, NY, USA: Simon and Schuster, 1988.

[3] R. Picard, *Affective Computing*. Cambridge, MA, USA: MIT Media Lab., 1995.

[4] P. Ekman et al., "Universals and cultural differences in the judgments of facial expressions of emotion," *J. Personality Social Psychol.*, vol. 53, no. 4, pp. 712–717, 1987.

[5] M. El Ayadi, M. S. Kamel, and F. Karray, "Survey on speech emotion recognition: Features, classification schemes, and databases," *Pattern Recognit.*, vol. 44, no. 3, pp. 572–587, Mar. 2011.

[6] M. Kipp and J.-C. Martin, "Gesture and emotion: Can basic gestural form features discriminate emotions?" in *Proc. 3rd Int. Conf. Affect. Comput. Intell. Interact. Workshops*, Amsterdam, The Netherlands, Sep. 2009, pp. 1–8.

[7] C. O. Alm, D. Roth, and R. Sproat, "Emotions from text: Machine learning for text-based emotion prediction," in *Proc. Conf. Hum. Lang. Technol. Empirical Methods Natural Lang. Process.*, Vancouver, BC, Canada, 2005, pp. 579–586.

[8] L. Kessous, G. Castellano, and G. Caridakis, "Multimodal emotion recognition in speech-based interaction using facial expression, body gesture and acoustic analysis," *J. Multimodal User Interfaces*, vol. 3, nos. 1–2, pp. 33–48, Mar. 2010.

[9] R. W. Picard, E. Vyzas, and J. Healey, "Toward machine emotional intelligence: Analysis of affective physiological state," *IEEE Trans. Pattern Anal. Mach. Intell.*, vol. 23, no. 10, pp. 1175–1191, Oct. 2001.

[10] X. Quan, Z. Zeng, J. Jiang, Y. Zhang, B.-L. Lv, and D. Wu, "Physiological signals based affective computing: A systematic review," *Acta Autom. Sinica*, vol. 47, no. 8, pp. 1769–1784, 2021.

[11] B. J. Lance, S. E. Kerick, A. J. Ries, K. S. Oie, and K. McDowell, "Brain–computer interface technologies in the coming decades," *Proc. IEEE*, vol. 100, no. 2, pp. 1585–1599, May 2012.

[12] J. J. Daly and J. R. Wolpaw, "Brain–computer interfaces in neurological rehabilitation," *Lancet Neurol.*, vol. 7, no. 11, pp. 1032–1043, 2008.

[13] X. Chen, Y. Wang, M. Nakanishi, X. Gao, T.-P. Jung, and S. Gao, "High-speed spelling with a noninvasive brain–computer interface," *Proc. Nat. Acad. Sci. USA*, vol. 112, no. 44, pp. E6058–E6067, Nov. 2015.

[14] D. Marshall, D. Coyle, S. Wilson, and M. Callaghan, "Games, gameplay, and BCI: The state of the art," *IEEE Trans. Comput. Intell. AI Games*, vol. 5, no. 2, pp. 82–99, Jun. 2013.

[15] H. Huang et al., "An EEG-based brain computer interface for emotion recognition and its

application in patients with disorder of consciousness," *IEEE Trans. Affect. Comput.*, vol. 12, no. 4, pp. 832–842, Oct. 2021.
[16] T. G. Monteiro, C. Skourup, and H. Zhang, "Using EEG for mental fatigue assessment: A comprehensive look into the current state of the art," *IEEE Trans. Hum.-Mach. Syst.*, vol. 49, no. 6, pp. 599–610, Dec. 2019.
[17] W.-L. Zheng and B.-L. Lu, "A multimodal approach to estimating vigilance using EEG and forehead EOG," *J. Neural Eng.*, vol. 14, no. 2, Apr. 2017, Art. no. 026017.
[18] G. K. Anumanchipalli, J. Chartier, and E. F. Chang, "Speech synthesis from neural decoding of spoken sentences," *Nature*, vol. 568, no. 7753, pp. 493–498, Apr. 2019.
[19] D. A. Moses et al., "Neuroprosthesis for decoding speech in a paralyzed person with anarthria," *New England J. Med.*, vol. 385, no. 3, pp. 217–227, Jul. 2021.
[20] M. Capogrosso et al., "A brain–spine interface alleviating gait deficits after spinal cord injury in primates," *Nature*, vol. 539, no. 7628, pp. 284–288, 2016.
[21] P. D. Ganzer et al., "Restoring the sense of touch using a sensorimotor demultiplexing neural interface," *Cell*, vol. 181, no. 4, pp. 763–773, May 2020.
[22] M. Velliste, S. Perel, M. C. Spalding, A. S. Whitford, and A. B. Schwartz, "Cortical control of a prosthetic arm for self-feeding," *Nature*, vol. 453, no. 7198, pp. 1098–1101, Jun. 2008.
[23] L. R. Hochberg et al., "Reach and grasp by people with tetraplegia using a neurally controlled robotic arm," *Nature*, vol. 485, no. 7398, pp. 372–375, May 2012.
[24] R. P. Rao, *Brain–Computer Interfacing: An Introduction*. New York, NY, USA: Cambridge Univ. Press, 2013.
[25] M. L. Martini, E. K. Oermann, N. L. Opie, F. Panov, T. Oxley, and K. Yaeger, "Sensor modalities for brain–computer interface technology: A comprehensive literature review," *Neurosurgery*, vol. 86, no. 2, pp. E108–E117, 2020.
[26] C. Muhl, B. Allison, A. Nijholt, and G. Chanel, "A survey of affective brain computer interfaces: Principles, state-of-the-art, and challenges," *Brain-Comput. Interfaces*, vol. 1, no. 2, pp. 66–84, Apr. 2014.
[27] M. M. Shanechi, "Brain–machine interfaces from motor to mood," *Nature Neurosci.*, vol. 22, no. 10, pp. 1554–1564, Oct. 2019.
[28] G. Pfurtscheller and C. Neuper, "Motor imagery and direct brain–computer communication," *Proc. IEEE*, vol. 89, no. 7, pp. 1123–1134, Jul. 2001.
[29] P. Ekman and W. V. Friesen, "Constants across cultures in the face and emotion.," *J. Personality Social Psychol.*, vol. 17, no. 2, pp. 124–129, 1971.
[30] J. A. Russell, "A circumplex model of affect," *J. Personality Social Psychol.*, vol. 39, no. 6, pp. 1161–1178, Dec. 1980.
[31] A. Mehrabian and J. A. Russell, *An Approach to Environmental Psychology*. Cambridge, MA, USA: MIT Press, 1974.
[32] G. Pfurtscheller, D. Flotzinger, and J. Kalcher, "Brain–computer interface—A new communication device for handicapped persons," *J. Microcomput. Appl.*, vol. 16, no. 3, pp. 293–299, Jul. 1993.
[33] L. A. Farwell and E. Donchin, "Talking off the top of your head: Toward a mental prosthesis utilizing event-related brain potentials," *Electroencephalogr. Clin. Neurophysiol.*, vol. 70, no. 6, pp. 510–523, Dec. 1988.
[34] O. Friman, I. Volosyak, and A. Graser, "Multiple channel detection of steady-state visual evoked potentials for brain–computer interfaces," *IEEE Trans. Biomed. Eng.*, vol. 54, no. 4, pp. 742–750, Apr. 2007.
[35] S. Koelstra et al., "DEAP: A database for emotion analysis; using physiological signals," *IEEE Trans. Affect. Comput.*, vol. 3, no. 1, pp. 18–31, Mar. 2012.
[36] L.-D. Liao et al., "Biosensor technologies for augmented brain–computer interfaces in the next decades," *Proc. IEEE*, vol. 100, no. 2, pp. 1553–1566, May 2012.
[37] P. Fattahi, G. Yang, G. Kim, and M. R. Abidian, "A review of organic and inorganic biomaterials for neural interfaces," *Adv. Mater.*, vol. 26, no. 12, pp. 1846–1885, Mar. 2014.
[38] *Electroencephalography*. Accessed: May 25, 2025. [Online]. Available: https://en.wikipedia.org/wiki/Electroencephalography
[39] B.-L. Lu, Y. Zhang, and W.-L. Zheng, "A survey of affective brain–computer interface," *Chin. J. Intell. Sci. Technol.*, vol. 3, no. 1, pp. 36–48, 2021.
[40] W. J. Ray and H. W. Cole, "EEG alpha activity reflects attentional demands, and beta activity reflects emotional and cognitive processes," *Science*, vol. 228, no. 4700, pp. 750–752, May 1985.
[41] W. Zheng, J. Zhu, and B. Lu, "Identifying stable patterns over time for emotion recognition from EEG," *IEEE Trans. Affect. Comput.*, vol. 10, no. 3, pp. 417–429, Jul. 2019.
[42] Y. Peng, F. Qin, W. Kong, Y. Ge, F. Nie, and A. Cichocki, "GFIL: A unified framework for the importance analysis of features, frequency bands, and channels in EEG-based emotion recognition," *IEEE Trans. Cognit. Develop. Syst.*, vol. 14, no. 3, pp. 935–947, Sep. 2022.
[43] S. A. Huettel et al., *Functional Magnetic Resonance Imaging*, vol. 1. Sunderland, MA, USA: Sinauer Associates, 2004.
[44] M. Ferrari and V. Quaresima, "A brief review on the history of human functional near-infrared spectroscopy (fNIRS) development and fields of application," *NeuroImage*, vol. 63, no. 2, pp. 921–935, Nov. 2012.
[45] M. Soleymani, J. Lichtenauer, T. Pun, and M. Pantic, "A multimodal database for affect recognition and implicit tagging," *IEEE Trans. Affect. Comput.*, vol. 3, no. 1, pp. 42–55, Mar. 2012.
[46] W. Zheng and B. Lu, "Investigating critical frequency bands and channels for EEG-based emotion recognition with deep neural networks," *IEEE Trans. Auto. Mental Develop.*, vol. 7, no. 3, pp. 162–175, Sep. 2015.
[47] R. Subramanian, J. Wache, M. K. Abadi, R. L. Vieriu, S. Winkler, and N. Sebe, "ASCERTAIN: Emotion and personality recognition using commercial sensors," *IEEE Trans. Affect. Comput.*, vol. 9, no. 2, pp. 147–160, Apr. 2018.
[48] S. Katsigiannis and N. Ramzan, "DREAMER: A database for emotion recognition through EEG and ECG signals from wireless low-cost off-the-shelf devices," *IEEE J. Biomed. Health Informat.*, vol. 22, no. 1, pp. 98–107, Jan. 2018.
[49] J. A. Miranda-Correa, M. K. Abadi, N. Sebe, and I. Patras, "AMIGOS: A dataset for affect, personality and mood research on individuals and groups," *IEEE Trans. Affect. Comput.*, vol. 12, no. 2, pp. 479–493, Apr. 2021.
[50] Y. Li, W. Zheng, Z. Cui, Y. Zong, and S. Ge, "EEG emotion recognition based on graph regularized sparse linear regression," *Neural Process. Lett.*, vol. 49, no. 2, pp. 555–571, Apr. 2019.
[51] T. Song, W. Zheng, C. Lu, Y. Zong, X. Zhang, and Z. Cui, "MPED: A multi-modal physiological emotion database for discrete emotion recognition," *IEEE Access*, vol. 7, pp. 12177–12191, 2019.
[52] W. Zheng, W. Liu, Y. Lu, B. Lu, and A. Cichocki, "EmotionMeter: A multimodal framework for recognizing human emotions," *IEEE Trans. Cybern.*, vol. 49, no. 3, pp. 1110–1122, Mar. 2019.
[53] H. Becker, J. Fleureau, P. Guillotel, F. Wendling, I. Merlet, and L. Albera, "Emotion recognition based on high-resolution EEG recordings and reconstructed brain sources," *IEEE Trans. Affect. Comput.*, vol. 11, no. 2, pp. 244–257, Apr. 2020.
[54] T. Li, W. Liu, W. Zheng, and B. Lu, "Classification of five emotions from EEG and eye movement signals: Discrimination ability and stability over time," in *Proc. 9th Int. IEEE/EMBS Conf. Neural Eng. (NER)*. San Francisco, CA, USA: IEEE, Mar. 2019, pp. 607–610.
[55] W. Liu, W.-L. Zheng, Z. Li, S.-Y. Wu, L. Gan, and B.-L. Lu, "Identifying similarities and differences in emotion recognition with EEG and eye movements among Chinese, German, and French people," *J. Neural Eng.*, vol. 19, no. 2, Apr. 2022, Art. no. 026012.
[56] J. Xue, J. Wang, S. Hu, N. Bi, and Z. Lv, "OVPD: Odor-video elicited physiological signal database for emotion recognition," *IEEE Trans. Instrum. Meas.*, vol. 71, pp. 1–12, 2022.
[57] D. Dinges and R. Grace, "PERCLOS: A valid psychophysiological measure of alertness as assessed by psychomotor vigilance," U.S. Dept. Transp., Federal Highway Admin., Oklahoma City, OK, USA, Tech. Rep., FHWA-MCRT-98-006, 1998.
[58] S. M. Alarcão and M. J. Fonseca, "Emotions recognition using EEG signals: A survey," *IEEE Trans. Affect. Comput.*, vol. 10, no. 3, pp. 374–393, Jul. 2019.
[59] M. Klug and K. Gramann, "Identifying key factors for improving ICA-based decomposition of EEG data in mobile and stationary experiments," *Eur. J. Neurosci.*, vol. 54, no. 12, pp. 8406–8420, 2021.
[60] *Backgound on EEG References*. Accessed: Sep. 25, 2022. [Online]. Available: https://eeglab.org/tutorials/ConceptsGuide/rereferencing_background.html
[61] S. Makeig, A. J. Bell, T.-P. Jung, and T. J. Sejnowski, "Independent component analysis of electroencephalographic data," in *Proc. Adv. Neural Inf. Process. Syst.*, Denver, CO, USA, Dec. 1996, pp. 145–151.
[62] T.-P. Jung et al., "Removing electroencephalographic artifacts by blind source separation," *Psychophysiology*, vol. 37, no. 2, pp. 163–178, Mar. 2000.
[63] S. B. Rutkove, *Introduction to Volume Conduction*. Totowa, NJ, USA: Humana Press, 2007, pp. 43–53.
[64] *Background on Independent Component Analysis Applied to EEG*. Accessed: Sep. 25, 2022. [Online]. Available: https://eeglab.org/tutorials/ConceptsGuide/ICA_background.html
[65] J. Yu, C. Li, K. Lou, C. Wei, and Q. Liu, "Embedding decomposition for artifacts removal in EEG signals," *J. Neural Eng.*, vol. 19, no. 2, Apr. 2022, Art. no. 026052.
[66] Y. Wang and D. Wu, "Real-time fMRI based brain computer interface: A review," in *Proc. 24th Int. Conf. Neural Inf. Process.*, Guangzhou, China, Nov. 2017, pp. 833–842.
[67] R. Sladky, K. J. Friston, J. Tröstl, R. Cunnington, E. Moser, and C. Windischberger, "Slice-timing effects and their correction in functional MRI," *NeuroImage*, vol. 58, no. 2, pp. 588–594, Sep. 2011.
[68] K. J. Friston, C. D. Frith, R. S. J. Frackowiak, and R. Turner, "Characterizing dynamic brain responses with fMRI: A multivariate approach," *NeuroImage*, vol. 2, no. 2, pp. 166–172, Jun. 1995.
[69] W. M. Wells, P. Viola, H. Atsumi, S. Nakajima, and R. Kikinis, "Multi-modal volume registration by maximization of mutual information," *Med. Image Anal.*, vol. 1, no. 1, pp. 35–51, Mar. 1996.
[70] J. Ashburner and K. Friston, "The role of registration and spatial normalisation in detecting activations in functional imaging," *Clin. MRI*, vol. 7, no. 1, pp. 26–27, 1997.
[71] P. Pinti, F. Scholkmann, A. Hamilton, P. Burgess, and I. Tachtsidis, "Current status and issues regarding pre-processing of fNIRS neuroimaging data: An investigation of diverse signal filtering methods within a general linear model framework," *Frontiers Hum. Neurosci.*, vol. 12, p. 505, Jan. 2019.
[72] M. L. Filippetti, J. Andreu-Perez, C. De Klerk, C. Richmond, and S. Rigato, "Are advanced methods necessary to improve infant fNIRS data analysis? An assessment of baseline-corrected averaging, general linear model (GLM) and multivariate pattern analysis (MVPA) based approaches," *NeuroImage*, vol. 265, Nov. 2023, Art. no. 119756.
[73] R. Jenke, A. Peer, and M. Buss, "Feature extraction and selection for emotion recognition from EEG,"

IEEE Trans. Affect. Comput., vol. 5, no. 3, pp. 327–339, Sep. 2014.
[74] Z. Mohammadi, J. Frounchi, and M. Amiri, "Wavelet-based emotion recognition system using EEG signal," *Neural Comput. Appl.*, vol. 28, no. 8, pp. 1985–1990, Aug. 2017.
[75] E. Kroupi, J. Vesin, and T. Ebrahimi, "Subject-independent odor pleasantness classification using brain and peripheral signals," *IEEE Trans. Affect. Comput.*, vol. 7, no. 4, pp. 422–434, Oct. 2016.
[76] B. Hjorth, "EEG analysis based on time domain properties," *Electroencephalogr. Clin. Neurophysiol.*, vol. 29, no. 3, pp. 306–310, Sep. 1970.
[77] J. M. Hausdorff, A. Lertratanakul, M. E. Cudkowicz, A. L. Peterson, D. Kaliton, and A. L. Goldberger, "Dynamic markers of altered gait rhythm in amyotrophic lateral sclerosis," *J. Appl. Physiol.*, vol. 88, no. 6, pp. 2045–2053, Jun. 2000.
[78] T. Higuchi, "Approach to an irregular time series on the basis of the fractal theory," *Phys. D, Nonlinear Phenomena*, vol. 31, no. 2, pp. 277–283, Jun. 1988.
[79] P. C. Petrantonakis and L. J. Hadjileontiadis, "Emotion recognition from EEG using higher order crossings," *IEEE Trans. Inf. Technol. Biomed.*, vol. 14, no. 2, pp. 186–197, Mar. 2010.
[80] R.-N. Duan, J.-Y. Zhu, and B.-L. Lu, "Differential entropy feature for EEG-based emotion classification," in *Proc. 6th Int. IEEE/EMBS Conf. Neural Eng. (NER)*, San Diego, CA, USA, Nov. 2013, pp. 81–84.
[81] S. A. Hosseini, M. A. Khalilzadeh, M. B. Naghibi-Sistani, and V. Niazmand, "Higher order spectra analysis of EEG signals in emotional stress states," in *Proc. 2nd Int. Conf. Inf. Technol. Comput. Sci.*, Kiev, Ukraine, Jul. 2010, pp. 60–63.
[82] L.-C. Shi, Y.-Y. Jiao, and B.-L. Lu, "Differential entropy feature for EEG-based vigilance estimation," in *Proc. 35th Annu. Int. Conf. IEEE Eng. Med. Biol. Soc. (EMBC)*, Osaka, Japan, Jul. 2013, pp. 6627–6630.
[83] Y.-P. Lin, Y.-H. Yang, and T.-P. Jung, "Fusion of electroencephalographic dynamics and musical contents for estimating emotional responses in music listening," *Frontiers Neurosci.*, vol. 8, p. 94, May 2014.
[84] J. S. Richman and J. R. Moorman, "Physiological time-series analysis using approximate entropy and sample entropy," *Amer. J. Physiol.-Heart Circulatory Physiol.*, vol. 278, no. 6, pp. H2039–H2049, Jun. 2000.
[85] C. Bandt and B. Pompe, "Permutation entropy: A natural complexity measure for time series," *Phys. Rev. Lett.*, vol. 88, no. 17, Apr. 2002, Art. no. 174102.
[86] M. Rostaghi and H. Azami, "Dispersion entropy: A measure for time-series analysis," *IEEE Signal Process. Lett.*, vol. 23, no. 5, pp. 610–614, May 2016.
[87] X. Ding, Z. Liu, D. Li, Y. He, and M. Wu, "Electroencephalogram emotion recognition based on dispersion entropy feature extraction using random oversampling imbalanced data processing," *IEEE Trans. Cognit. Develop. Syst.*, vol. 14, no. 3, pp. 882–891, Sep. 2022.
[88] G. Giannakakis, D. Grigoriadis, K. Giannakaki, O. Simantiraki, A. Roniotis, and M. Tsiknakis, "Review on psychological stress detection using biosignals," *IEEE Trans. Affect. Comput.*, vol. 13, no. 1, pp. 440–460, Jan. 2022.
[89] S. K. Hadjidimitriou and L. J. Hadjileontiadis, "EEG-based classification of music appraisal responses using time-frequency analysis and familiarity ratings," *IEEE Trans. Affect. Comput.*, vol. 4, no. 2, pp. 161–172, Jun. 2013.
[90] M. Murugappan, M. Rizon, R. Nagarajan, S. Yaacob, I. Zunaidi, and D. Hazry, "EEG feature extraction for classifying emotions using FCM and FKM," *Int. J. Comput. Commun.*, vol. 1, no. 2, pp. 21–25, 2007.
[91] L. Cohen, "Time-frequency distributions—A review," *Proc. IEEE*, vol. 77, no. 7, pp. 941–981, Jul. 1989.
[92] Y. Zhao, L. E. Atlas, and R. J. Marks, "The use of cone-shaped kernels for generalized time-frequency representations of nonstationary signals," *IEEE Trans. Acoust., Speech, Signal Process.*, vol. 38, no. 7, pp. 1084–1091, Jul. 1990.
[93] N. Huang et al., "The empirical modedecomposition and the Hilbert spectrum for nonlinear and non-stationary time series analysis," *Proc. Roy. Soc. London. Ser. A, Math., Phys. Eng. Sci.*, vol. 454, no. 1971, pp. 903–995, 1998.
[94] P. C. Petrantonakis and L. J. Hadjileontiadis, "Emotion recognition from brain signals using hybrid adaptive filtering and higher order crossings analysis," *IEEE Trans. Affect. Comput.*, vol. 1, no. 2, pp. 81–97, Dec. 2010.
[95] S. Moon, S. Jang, and J. Lee, "Convolutional neural network approach for EEG-based emotion recognition using brain connectivity and its spatial information," in *Proc. IEEE Int. Conf. Acoust., Speech Signal Process. (ICASSP)*, Calgary, AB, Canada, Apr. 2018, pp. 2556–2560.
[96] J.-P. Lachaux, E. Rodriguez, J. Martinerie, and F. J. Varela, "Measuring phase synchrony in brain signals," *Hum. Brain Mapping*, vol. 8, no. 4, pp. 194–208, 1999.
[97] C. J. Stam, G. Nolte, and A. Daffertshofer, "Phase lag index: Assessment of functional connectivity from multi channel EEG and MEG with diminished bias from common sources," *Hum. Brain Mapping*, vol. 28, no. 11, pp. 1178–1193, 2007.
[98] S. Liu, X. Wang, L. Zhao, J. Zhao, Q. Xin, and S. Wang, "Subject-independent emotion recognition of EEG signals based on dynamic empirical convolutional neural network," *IEEE/ACM Trans. Comput. Biol. Bioinf.*, vol. 18, no. 5, pp. 1710–1721, Sep. 2021.
[99] J. Zhang et al., "Disrupted brain connectivity networks in drug-naive, first-episode major depressive disorder," *Biol. Psychiatry*, vol. 70, no. 4, pp. 334–342, Aug. 2011.
[100] J. Han, X. Ji, X. Hu, L. Guo, and T. Liu, "Arousal recognition using audio-visual features and FMRI-based brain response," *IEEE Trans. Affect. Comput.*, vol. 6, no. 4, pp. 337–347, Oct. 2015.
[101] N. Tzourio-Mazoyer et al., "Automated anatomical labeling of activations in SPM using a macroscopic anatomical parcellation of the MNI MRI single-subject brain," *NeuroImage*, vol. 15, no. 1, pp. 273–289, Jan. 2002.
[102] D. Zhu et al., "DICCCOL: Dense individualizedand common connectivity-based cortical landmarks," *Cerebral cortex*, vol. 23, no. 4, pp. 786–800, 2013.
[103] D. Watts and S. Strogatz, "Collective dynamics of 'small-world' networks," *Nature*, vol. 393, pp. 440–442, Jun. 1998.
[104] V. Latora and M. Marchiori, "Efficient behavior of small-world networks," *Phys. Rev. Lett.*, vol. 87, Oct. 2001, Art. no. 198701.
[105] M. Rubinov and O. Sporns, "Complex network measures of brain connectivity: Uses and interpretations," *NeuroImage*, vol. 52, no. 3, pp. 1059–1069, Sep. 2010.
[106] Y. Sun, H. Ayaz, and A. N. Akansu, "Multimodal affective state assessment using fNIRS + EEG and spontaneous facial expression," *Brain Sci.*, vol. 10, no. 2, p. 85, Feb. 2020.
[107] H. Cai, Z. Qu, Z. Li, Y. Zhang, X. Hu, and B. Hu, "Feature-level fusion approaches based on multimodal EEG data for depression recognition," *Inf. Fusion*, vol. 59, pp. 127–138, Jul. 2020.
[108] D. Wu et al., "Optimal arousal identification and classification for affective computing using physiological signals: Virtual reality Stroop task," *IEEE Trans. Affect. Comput.*, vol. 1, no. 2, pp. 109–118, Jul. 2010.
[109] Z. Liang et al., "EEGFuseNet: Hybrid unsupervised deep feature characterization and fusion for high-dimensional EEG with an application to emotion recognition," *IEEE Trans. Neural Syst. Rehabil. Eng.*, vol. 29, pp. 1913–1925, 2021.
[110] B. García-Martínez, A. Martínez-Rodrigo, R. Alcaraz, and A. Fernández-Caballero, "A review on nonlinear methods using electroencephalographic recordings for emotion recognition," *IEEE Trans. Affect. Comput.*, vol. 12, no. 3, pp. 801–820, Jul. 2021.
[111] S. Liu et al., "3DCANN: A spatio-temporal convolution attention neural network for EEG emotion recognition," *IEEE J. Biomed. Health Informat.*, vol. 26, no. 11, pp. 5321–5331, Nov. 2022.
[112] F. Wang et al., "Emotion recognition with convolutional neural network and EEG-based EFDMs," *Neuropsychologia*, vol. 146, Sep. 2020, Art. no. 107506.
[113] X. Wu, W.-L. Zheng, Z. Li, and B.-L. Lu, "Investigating EEG-based functional connectivity patterns for multimodal emotion recognition," *J. Neural Eng.*, vol. 19, no. 1, Feb. 2022, Art. no. 016012.
[114] Y. Luo et al., "EEG-based emotion classification using spiking neural networks," *IEEE Access*, vol. 8, pp. 46007–46016, 2020.
[115] R. Li et al., "The perils and pitfalls of block design for EEG classification experiments," *IEEE Trans. Pattern Anal. Mach. Intell.*, vol. 43, no. 1, pp. 316–333, Jan. 2021.
[116] F. Zhuang et al., "A comprehensive survey on transfer learning," *Proc. IEEE*, vol. 109, no. 1, pp. 1–34, Jul. 2020.
[117] D. Wu, Y. Xu, and B. Lu, "Transfer learning for EEG-based brain–computer interfaces: A review of progress made since 2016," *IEEE Trans. Cognit. Develop. Syst.*, vol. 14, no. 1, pp. 4–19, Mar. 2022.
[118] W. Zhang, L. Deng, L. Zhang, and D. Wu, "A survey on negative transfer," *IEEE/CAA J. Autom. Sinica*, vol. 10, no. 2, pp. 305–329, Feb. 2023.
[119] X. Zhang et al., "Individual similarity guided transfer modeling for EEG-based emotion recognition," in *Proc. IEEE Int. Conf. Bioinf. Biomed. (BIBM)*, San Diego, CA, USA, Nov. 2019, pp. 1156–1161.
[120] Y. Lin, "Constructing a personalized cross-day EEG-based emotion-classification model using transfer learning," *IEEE J. Biomed. Health Informat.*, vol. 24, no. 5, pp. 1255–1264, May 2020.
[121] W. Zheng, Y. Zhang, J. Zhu, and B. Lu, "Transfer components between subjects for EEG-based emotion recognition," in *Proc. Int. Conf. Affect. Comput. Intell. Interact. (ACII)*, Xian, China, Sep. 2015, pp. 917–922.
[122] S. Jialin Pan, I. W. Tsang, J. T. Kwok, and Q. Yang, "Domain adaptation via transfer component analysis," *IEEE Trans. Neural Netw.*, vol. 22, no. 2, pp. 199–210, Feb. 2011.
[123] B. Schölkopf, A. Smola, and K.-R. Müller, "Nonlinear component analysis as a kernel eigenvalue problem," *Neural Comput.*, vol. 10, no. 5, pp. 1299–1319, Jul. 1998.
[124] X. Chai et al., "A fast, efficient domain adaptation technique for cross-domain electroencephalography(EEG)-based emotion recognition," *Sensors*, vol. 17, no. 5, p. 1014, May 2017.
[125] P. Zanini, M. Congedo, C. Jutten, S. Said, and Y. Berthoumieu, "Transfer learning: A Riemannian geometry framework with applications to brain–computer interfaces," *IEEE Trans. Biomed. Eng.*, vol. 65, no. 5, pp. 1107–1116, May 2018.
[126] H. He and D. Wu, "Transfer learning for brain–computer interfaces: A Euclidean space data alignment approach," *IEEE Trans. Biomed. Eng.*, vol. 67, no. 2, pp. 399–410, Feb. 2020.
[127] Y. Wang, J. Liu, Q. Ruan, S. Wang, and C. Wang, "Cross-subject EEG emotion classification based on few-label adversarial domain adaption," *Exp. Syst. Appl.*, vol. 185, Dec. 2021, Art. no. 115581.
[128] Y. Jiang, S. Xie, X. Xie, Y. Cui, and H. Tang, "Emotion recognition via multiscale feature fusion network and attention mechanism," *IEEE Sensors J.*, vol. 23, no. 10, pp. 10790–10800, May 2023.
[129] W.-L. Zheng and B.-L. Lu, "Personalizing EEG-based affective models with transfer learning," in *Proc. 25th Int. Joint Conf. Artif. Intell.*, New York, NY, USA, Jul. 2016, pp. 2732–2738.
[130] W. Li, W. Huan, B. Hou, Y. Tian, Z. Zhang, and A. Song, "Can emotion be transferred?—A review on transfer learning for EEG-based emotion

recognition," *IEEE Trans. Cognit. Develop. Syst.*, vol. 14, no. 3, pp. 833–846, Jul. 2022.
[131] J. Li, S. Qiu, Y. Shen, C. Liu, and H. He, "Multisource transfer learning for cross-subject EEG emotion recognition," *IEEE Trans. Cybern.*, vol. 50, no. 7, pp. 3281–3293, Jul. 2020.
[132] I. Goodfellow, Y. Bengio, and A. Courville, *Deep Learning*. Boston, MA, USA: MIT Press, 2016. [Online]. Available: http://www.deeplearningbook.org
[133] Y. Luo, S.-Y. Zhang, W.-L. Zheng, and B.-L. Lu, "WGAN domain adaptation for EEG-based emotion recognition," in *Proc. Int. Conf. Neural Inf. Process.*, Siem Reap, Cambodia, Dec. 2018, pp. 275–286.
[134] D. Ruta and B. Gabrys, "An overview of classifier fusion methods," *Comput. Inf. Syst.*, vol. 7, no. 1, pp. 1–10, 2000.
[135] Y. Huang, J. Yang, P. Liao, and J. Pan, "Fusion of facial expressions and EEG for multimodal emotion recognition," *Comput. Intell. Neurosci.*, vol. 2017, Sep. 2017, Art. no. 2107451.
[136] W.-L. Zheng, B.-N. Dong, and B.-L. Lu, "Multimodal emotion recognition using EEG and eye tracking data," in *Proc. 36th Annu. Int. Conf. IEEE Eng. Med. Biol. Soc.*, Chicago, IL, USA, Aug. 2014, pp. 5040–5043.
[137] M. Soleymani, M. Pantic, and T. Pun, "Multimodal emotion recognition in response to videos," *IEEE Trans. Affect. Comput.*, vol. 3, no. 2, pp. 211–223, Jun. 2012.
[138] W.-L. Zheng, Z.-F. Shi, and B.-L. Lu, "Building cross-subject EEG-based affective models using heterogeneous transfer learning," *Chin. J. Comput.*, vol. 43, no. 2, pp. 177–189, 2020, in Chinese.
[139] X. Yan, L.-M. Zhao, and B.-L. Lu, "Simplifying multimodal emotion recognition with single eye movement modality," in *Proc. 29th ACM Int. Conf. Multimedia*, Oct. 2021, pp. 1057–1063.
[140] F. Wang, M. Mao, L. Duan, Y. Huang, Z. Li, and C. Zhu, "Intersession instability in fNIRS-based emotion recognition," *IEEE Trans. Neural Syst. Rehabil. Eng.*, vol. 26, no. 7, pp. 1324–1333, Jul. 2018.
[141] A. Etkin, C. Büchel, and J. J. Gross, "The neural bases of emotion regulation," *Nature Rev. Neurosci.*, vol. 16, no. 11, pp. 693–700, Nov. 2015.
[142] W. Huang, W. Wu, M. V. Lucas, H. Huang, Z. Wen, and Y. Li, "Neurofeedback training with an electroencephalogram-based brain–computer interface enhances emotion regulation," *IEEE Trans. Affect. Comput.*, early access, Dec. 13, 2021, doi: 10.1109/TAFFC.2021.3134183.
[143] J. V. Hardt and J. Kamiya, "Anxiety change through electroencephalographic alpha feedback seen only in high anxiety subjects," *Science*, vol. 201, no. 4350, pp. 79–81, Jul. 1978.
[144] R. Mennella, E. Patron, and D. Palomba, "Frontal alpha asymmetry neurofeedback for the reduction of negative affect and anxiety," *Behaviour Res. Therapy*, vol. 92, pp. 32–40, May 2017.
[145] P. Linhartová, A. Látalová, B. Kósa, T. Kaspárek, C. Schmahl, and C. Paret, "FMRI neurofeedback in emotion regulation: A literature review," *NeuroImage*, vol. 193, pp. 75–92, Jun. 2019.
[146] A.-C.-S. Kimmig et al., "Feasibility of NIRS-based neurofeedback training in social anxiety disorder: Behavioral and neural correlates," *J. Neural Transmiss.*, vol. 126, no. 9, pp. 1175–1185, Sep. 2019.
[147] C. Cusin and D. D. Dougherty, "Somatic therapies for treatment-resistant depression: ECT, TMS, VNS, DBS," *Biol. Mood Anxiety Disorders*, vol. 2, no. 1, pp. 1–9, Dec. 2012.
[148] P. Antonenko, F. Paas, R. Grabner, and T. van Gog, "Using electroencephalography to measure cognitive load," *Educ. Psychol. Rev.*, vol. 22, no. 4, pp. 425–438, Dec. 2010.
[149] G. Du, W. Zhou, C. Li, D. Li, and P. X. Liu, "An emotion recognition method for game evaluation based on electroencephalogram," *IEEE Trans. Affect. Comput.*, vol. 14, no. 1, pp. 591–602, Jan. 2023.
[150] C. D. Wickens, "Multiple resources and performance prediction," *Theor. Issues Ergonom. Sci.*, vol. 3, no. 2, pp. 159–177, Jan. 2002.
[151] R. M. Yerkes and J. D. Dodson, "The relation of strength of stimulus to rapidity of habit-formation," *J. Comparative Neurol. Psychol.*, vol. 18, no. 5, pp. 459–482, Nov. 1908.
[152] A.-M. Brouwer, M. A. Hogervorst, J. B. F. van Erp, T. Heffelaar, P. H. Zimmerman, and R. Oostenveld, "Estimating workload using EEG spectral power and ERPs in the n-back task," *J. Neural Eng.*, vol. 9, no. 4, Aug. 2012, Art. no. 045008.
[153] C. Muhl, C. Jeunet, and F. Lotte, "EEG-based workload estimation across affective contexts," *Frontiers Neurosci.*, vol. 8, p. 114, Jun. 2014.
[154] Y. Zhou, S. Huang, Z. Xu, P. Wang, X. Wu, and D. Zhang, "Cognitive workload recognition using EEG signals and machine learning: A review," *IEEE Trans. Cognit. Develop. Syst.*, vol. 14, no. 3, pp. 799–818, Sep. 2022.
[155] P. Aricò et al., "Adaptive automation triggered by EEG-based mental workload index: A passive brain–computer interface application in realistic air traffic control environment," *Frontiers Hum. Neurosci.*, vol. 10, p. 539, Oct. 2016.
[156] L. Zhang et al., "Cognitive load measurement in a virtual reality-based driving system for autism intervention," *IEEE Trans. Affect. Comput.*, vol. 8, no. 2, pp. 176–189, Apr. 2017.
[157] *Fatality Analysis Reporting System Encyclopedia. National Highway Traffic Safety Administration*. Accessed: Feb. 2, 2017. [Online]. Available: https://www-fars.nhtsa.dot.gov/Main/index.aspx
[158] L. Bergasa, J. Nuevo, M. Sotelo, R. Barea, and M. Lopez, "Real-time system for monitoring driver vigilance," *IEEE Trans. Intell. Transp. Syst.*, vol. 7, no. 1, pp. 63–67, Mar. 2006.
[159] Y. Cui, Y. Xu, and D. Wu, "EEG-based driver drowsiness estimation using feature weighted episodic training," *IEEE Trans. Neural Syst. Rehabil. Eng.*, vol. 27, no. 11, pp. 2263–2273, Nov. 2019.
[160] D. Wu, V. J. Lawhern, S. Gordon, B. J. Lance, and C. Lin, "Driver drowsiness estimation from EEG signals using online weighted adaptation regularization for regression (OwARR)," *IEEE Trans. Fuzzy Syst.*, vol. 25, no. 6, pp. 1522–1535, Dec. 2017.
[161] C.-S. Wei, Y.-P. Lin, Y.-T. Wang, C.-T. Lin, and T.-P. Jung, "A subject-transfer framework for obviating inter- and intra-subject variability in EEG-based drowsiness detection," *NeuroImage*, vol. 174, pp. 407–419, 2018.
[162] *Depression*. Accessed: Oct. 1, 2022. [Online]. Available: https://www.who.int/news-room/fact-sheets/detail/depression
[163] J. J. Allen, W. G. Iacono, R. A. Depue, and P. Arbisi, "Regional electroencephalographic asymmetries in bipolar seasonal affective disorder before and after exposure to bright light," *Biol. Psychiatry*, vol. 33, nos. 8–9, pp. 642–646, Apr. 1993.
[164] K. M. Putnam and L. B. McSweeney, "Depressive symptoms and baseline prefrontal EEG alpha activity: A study utilizing ecological momentary assessment," *Biol. Psychol.*, vol. 77, no. 2, pp. 237–240, Feb. 2008.
[165] J. Li, Y. Hao, W. Zhang, X. Li, and B. Hu, "Effective connectivity based EEG revealing the inhibitory deficits for distracting stimuli in major depression disorders," *IEEE Trans. Affect. Comput.*, vol. 14, no. 1, pp. 694–705, Jan. 2023.
[166] F. S. De Aguiar Neto and J. L. G. Rosa, "Depression biomarkers using non-invasive EEG: A review," *Neurosci. Biobehavioral Rev.*, vol. 105, pp. 83–93, Oct. 2019.
[167] J. S. Perlmutter and J. W. Mink, "Deep brain stimulation," *Annu. Rev. Neurosci.*, vol. 29, p. 229, Jul. 2006.
[168] K. W. Scangos, G. S. Makhoul, L. P. Sugrue, E. F. Chang, and A. D. Krystal, "State-dependent responses to intracranial brain stimulation in a patient with depression," *Nature Med.*, vol. 27, no. 2, pp. 229–231, Feb. 2021.
[169] V. R. Rao et al., "Direct electrical stimulation of lateral orbitofrontal cortex acutely improves mood in individuals with symptoms of depression," *Current Biol.*, vol. 28, no. 24, pp. 3893–3902, Dec. 2018.
[170] F. Iacopi and C.-T. Lin, "A perspective on electroencephalography sensors for brain–computer interfaces," *Prog. Biomed. Eng.*, vol. 4, no. 4, Oct. 2022, Art. no. 043002.
[171] J. Deng, W. Dong, R. Socher, L.-J. Li, K. Li, and L. Fei-Fei, "ImageNet: A large-scale hierarchical image database," in *Proc. IEEE Conf. Comput. Vis. Pattern Recognit.*, Miami Beach, FL, USA, Jun. 2009, pp. 248–255.
[172] *GPT-3*. Accessed: Oct. 1, 2022. [Online]. Available: https://en.wikipedia.org/wiki/GPT-3
[173] *Data and Statistics on Children's Mental Health*. Accessed: Oct. 1, 2022. [Online]. Available: https://www.cdc.gov/childrensmentalhealth/data.html
[174] K. Xia et al., "Privacy-preserving brain–computer interfaces: A systematic review," *IEEE Trans. Computat. Social Syst.*, early access, Jun. 27, 2023, doi: 10.1109/TCSS.2022.3184818.
[175] X. Kong, W. Kong, Q. Fan, Q. Zhao, and A. Cichocki, "Task-independent EEG identification via low-rank matrix decomposition," in *Proc. IEEE Int. Conf. Bioinf. Biomed. (BIBM)*, Dec. 2018, pp. 412–419.
[176] R. Yuste et al., "Four ethical piorities for neurotechnologies and AI," *Nature*, vol. 551, no. 7679, pp. 159–163, 2017.
[177] M. Ienca, P. Haselager, and E. J. Emanuel, "Brain leaks and consumer neurotechnology," *Nature Biotechnol.*, vol. 36, no. 9, pp. 805–810, Oct. 2018.
[178] A. Agarwal et al., "Protecting privacy of users in brain–computer interface applications," *IEEE Trans. Neural Syst. Rehabil. Eng.*, vol. 27, no. 8, pp. 1546–1555, Aug. 2019.
[179] W. Zhang, Z. Wang, and D. Wu, "Multi-source decentralized transfer for privacy-preserving BCIs," *IEEE Trans. Neural Syst. Rehabil. Eng.*, vol. 30, pp. 2710–2720, 2022.
[180] D. J. Miller, Z. Xiang, and G. Kesidis, "Adversarial learning targeting deep neural network classification: A comprehensive review of defenses against attacks," *Proc. IEEE*, vol. 108, no. 3, pp. 402–433, Mar. 2020.
[181] X. Zhang and D. Wu, "On the vulnerability of CNN classifiers in EEG-based BCIs," *IEEE Trans. Neural Syst. Rehabil. Eng.*, vol. 27, no. 5, pp. 814–825, May 2019.
[182] Z. Liu, L. Meng, X. Zhang, W. Fang, and D. Wu, "Universal adversarial perturbations for CNN classifiers in EEG-based BCIs," *J. Neural Eng.*, vol. 18, no. 4, Aug. 2021, Art. no. 0460a4.
[183] X. Zhang et al., "Tiny noise, big mistakes: Adversarial perturbations induce errors in brain–computer interface spellers," *Nat. Sci. Rev.*, vol. 8, no. 4, Apr. 2021, Art. no. nwaa233.
[184] R. Bian, L. Meng, and D. Wu, "SSVEP-based brain–computer interfaces are vulnerable to square wave attacks," *Sci. China Inf. Sci.*, vol. 65, no. 4, Apr. 2022, Art. no. 140406.
[185] X. Jiang, L. Meng, S. Li, and D. Wu, "Active poisoning: Efficient backdoor attacks to transfer learning based BCIs," *Sci. China Inf. Sci.*, 2023. [Online]. Available: https://www.sciengine.com/SCIS/doi/10.1007/s11432-022-3548-2
[186] L. Meng, C.-T. Lin, T.-P. Jung, and D. Wu, "White-box target attack for EEG-based BCI regression problems," in *Proc. Int. Conf. Neural Inf. Process.*, Sydney, NSW, Australia, Dec. 2019, pp. 476–488.
[187] A. Binnendijk, T. Marler, and E. M. Bartels, *Brain–Computer Interfaces: U.S. Military Applications and Implications, An Initial Assessment*. Santa Monica, CA, USA: RAND Corporation, 2020.
[188] D. Wu et al., "Adversarial attacks and defenses in physiological computing: A systematic review," *Nat. Sci. Open*, vol. 2, no. 1, Jan. 2023, Art. no. 20220023.
[189] C. Szegedy et al., "Intriguing properties of neural networks," in *Proc. Int. Conf. Learn. Represent.*, Apr. 2014, pp. 1–10.
[190] N. Das et al., "Keeping the bad guys out:

Protecting and vaccinating deep learning with JPEG compression," 2017, *arXiv:1705.02900*.

[191] C. Xie, J. Wang, Z. Zhang, Y. Zhou, L. Xie, and A. Yuille, "Adversarial examples for semantic segmentation and object detection," in *Proc. IEEE Int. Conf. Comput. Vis. (ICCV)*, Oct. 2017, pp. 1369–1378.

[192] B. Biggio, B. Nelson, and P. Laskov, "Support vector machines under adversarial label noise," in *Proc. Asian Conf. Mach. Learn.*, Taipei, Taiwan, Nov. 2011, pp. 97–112.

[193] N. Papernot, P. McDaniel, X. Wu, S. Jha, and A. Swami, "Distillation as a defense to adversarial perturbations against deep neural networks," in *Proc. IEEE Symp. Secur. Privacy (SP)*, San Jose, CA, USA, May 2016, pp. 582–597.

[194] A. Qayyum, J. Qadir, M. Bilal, and A. Al-Fuqaha, "Secure and robust machine learning for healthcare: A survey," *IEEE Rev. Biomed. Eng.*, vol. 14, pp. 156–180, 2021.

ABOUT THE AUTHORS

Dongrui Wu (Fellow, IEEE) received the B.E. degree in automatic control from the University of Science and Technology of China, Hefei, China, in 2003, the M.E. degree in electrical engineering from the National University of Singapore, Singapore, in 2005, and the Ph.D. degree in electrical engineering from the University of Southern California, Los Angeles, CA, USA, in 2009.

He is currently a Professor with the School of Artificial Intelligence and Automation, Huazhong University of Science and Technology, Wuhan, China. He has more than 200 publications. His research interests include affective computing, brain–computer interface, computational intelligence, and machine learning.

Prof. Wu received the NAFIPS Early Career Award in 2014, the IEEE SMC Society Early Career Award in 2017, the USERN Prize in Formal Sciences in 2020, the Chinese Association of Automation Early Career Award in 2021, the Ministry of Education Young Scientist Award in 2022, and six Outstanding Paper Awards. He has been the Editor-in-Chief of IEEE TRANSACTIONS ON FUZZY SYSTEMS since 2023.

Bao-Liang Lu (Fellow, IEEE) received the B.S. degree in instrument and control engineering from the Qingdao University of Science and Technology, Qingdao, China, in 1982, the M.S. degree in computer science and technology from Northwestern Polytechnical University, Xi'an, China, in 1989, and the Dr.Eng. degree in electrical engineering from Kyoto University, Kyoto, Japan, in 1994.

He was with the Qingdao University of Science and Technology from 1982 to 1986. From 1994 to 1999, he was a Frontier Researcher with the Bio-Mimetic Control Research Center, Institute of Physical and Chemical Research (RIKEN), Nagoya, Japan, and a Research Scientist with the RIKEN Brain Science Institute, Wako, Japan, from 1999 to 2002. Since 2002, he has been a Full Professor with the Department of Computer Science and Engineering, Shanghai Jiao Tong University, Shanghai, China. He is an Executive Dean of the Qing Yuan Research Institute, Shanghai Jiao Tong University, where he is also the Director of the Center for Brain-Like Computing and Machine Intelligence, the Key Laboratory of Shanghai Education Commission Intelligent Interaction and Cognitive Engineering, and the Ruijin-Mihoyo Laboratory. His research interests include brain-like computing, deep learning, emotion artificial intelligence, and affective brain–computer interface.

Prof. Lu received the 2018 IEEE TRANSACTIONS ON AUTONOMOUS MENTAL DEVELOPMENT Outstanding Paper Award, the First Prize of the 10th Wu Wenjun Artificial Intelligence Natural Science Award, the 2021 Best of IEEE TRANSACTIONS ON AFFECTIVE COMPUTING Paper Collection, and the 2022 ANNS (Asia Pacific Neural Network Society) Outstanding Achievement Award. He was the Past President of the Asia Pacific Neural Network Assembly and the General Chair of the 18th International Conference on Neural Information Processing. He is an Associate Editor of IEEE TRANSACTIONS ON COGNITIVE AND DEVELOPMENTAL SYSTEMS, IEEE TRANSACTIONS ON AFFECTIVE COMPUTING, and the *Journal of Neural Engineering*.

Bin Hu (Fellow, IEEE) received the Ph.D. degree in computer science from the Institute of Computing Technology, Chinese Academy of Sciences, Beijing, China, in 1998.

He is currently a Professor and the Dean of the School of Medical Technology, Beijing Institute of Technology, Beijing. He has more than 400 publications (more than 10 000 citations; H-index: 51).

Prof. Hu is a member of the National Computer Science Teaching and Steering Committee and the Science and Technology Committee. He is a member of the Steering Council of Association for Computing Machinery (ACM) China. His awards include the 2014 China Overseas Innovation Talent Award, the 2016 Chinese Ministry of Education Technology Invention Award, the 2018 Chinese National Technology Invention Award, and the 2019 WIPO-CNIPA Award for Chinese Outstanding Patented Invention. He is a National Distinguished Expert and a 973 Chief Scientist, and was awarded National Advanced Worker in 2020. He is a Principal Investigator of large grants, such as the National Transformative Technology "Early Recognition and Intervention Technology of Mental Disorders Based on Psychophysiological Multimodal Information," which has greatly promoted the development of objective, quantitative diagnosis, and nondrug interventions for mental disorders. He is the Vice-Chair of the China Committee of the International Society for Social Neuroscience and the Co-Chair of the Computational Psychophysiology and Cognitive Computing Technical Committees of the IEEE Systems, Man and Cybernetics Society. He also serves as the Editor-in-Chief of IEEE TRANSACTIONS ON COMPUTATIONAL SOCIAL SYSTEMS.

Zhigang Zeng (Fellow, IEEE) received the Ph.D. degree in systems analysis and integration from the Huazhong University of Science and Technology, Wuhan, China, in 2003.

He is currently a Professor with the School of Artificial Intelligence and Automation, Huazhong University of Science and Technology, and the Key Laboratory of Image Processing and Intelligent Control of the Education Ministry of China, Wuhan. He has published over 300 international journal articles. His current research interests include the theory of functional differential equations and differential equations with discontinuous right-hand sides, and their applications to the dynamics of neural networks, memristive systems, and associative memories.

Dr. Zeng has been a member of the Editorial Board of *Neural Networks* since 2012, *Cognitive Computation* since 2010, and *Applied Soft Computing* since 2013. He was an Associate Editor of IEEE TRANSACTIONS ON NEURAL NETWORKS AND LEARNING SYSTEMS from 2010 to 2011 and IEEE TRANSACTIONS ON FUZZY SYSTEMS from 2016 to 2021. He has been an Associate Editor of IEEE TRANSACTIONS ON CYBERNETICS since 2014.